



TECH BRIEFS

NATIONAL AERONAUTICS AND SPACE ADMINISTRATION

-  **Technology Focus**
-  **Electronics/Computers**
-  **Software**
-  **Materials**
-  **Mechanics**
-  **Machinery/Automation**
-  **Manufacturing**
-  **Bio-Medical**
-  **Physical Sciences**
-  **Information Sciences**
-  **Books and Reports**

INTRODUCTION

Tech Briefs are short announcements of innovations originating from research and development activities of the National Aeronautics and Space Administration. They emphasize information considered likely to be transferable across industrial, regional, or disciplinary lines and are issued to encourage commercial application.

Availability of NASA Tech Briefs and TSPs

Requests for individual Tech Briefs or for Technical Support Packages (TSPs) announced herein should be addressed to

National Technology Transfer Center

Telephone No. (800) 678-6882 or via World Wide Web at www2.nttc.edu/leads/

Please reference the control numbers appearing at the end of each Tech Brief. Information on NASA's Commercial Technology Team, its documents, and services is also available at the same facility or on the World Wide Web at www.nctn.hq.nasa.gov.

Commercial Technology Offices and Patent Counsels are located at NASA field centers to provide technology-transfer access to industrial users. Inquiries can be made by contacting NASA field centers and program offices listed below.

NASA Field Centers and Program Offices

Ames Research Center

Carolina Blake
(650) 604-1754
carolina.m.blake@nasa.gov

Dryden Flight Research Center

Jenny Baer-Riedhart
(661) 276-3689
jenny.baer-riedhart@dfrc.nasa.gov

Goddard Space Flight Center

Nona Cheeks
(301) 286-5810
Nona.K.Cheeks.1@gssc.nasa.gov

Jet Propulsion Laboratory

Art Murphy, Jr.
(818) 354-3480
arthur.j.murphy-jr@jpl.nasa.gov

Johnson Space Center

Charlene E. Gilbert
(281) 483-3809
commercialization@jsc.nasa.gov

Kennedy Space Center

Jim Aliberti
(321) 867-6224
Jim.Aliberti-1@ksc.nasa.gov

Langley Research Center

Jesse Midgett
(757) 864-3936
jesse.c.midgett@nasa.gov

John H. Glenn Research Center at Lewis Field

Larry Viterna
(216) 433-3484
cto@grc.nasa.gov

Marshall Space Flight Center

Vernotto McMillan
(256) 544-2615
vernotto.mcmillan@msfc.nasa.gov

Stennis Space Center

Robert Bruce
(228) 688-1929
robert.c.bruce@nasa.gov

NASA Program Offices

At NASA Headquarters there are seven major program offices that develop and oversee technology projects of potential interest to industry:

Carl Ray

Small Business Innovation Research Program (SBIR) & Small Business Technology Transfer Program (STTR)
(202) 358-4652 or
cray@mail.hq.nasa.gov

Benjamin Neumann

Innovative Technology Transfer Partnerships (Code RP)
(202) 358-2320
benjamin.j.neumann@nasa.gov

John Mankins

Office of Space Flight (Code MP)
(202) 358-4659 or
jmankins@mail.hq.nasa.gov

Terry Hertz

Office of Aero-Space Technology (Code RS)
(202) 358-4636 or
thertz@mail.hq.nasa.gov

Glen Mucklow

Office of Space Sciences (Code SM)
(202) 358-2235 or
gmucklow@mail.hq.nasa.gov

Roger Crouch

Office of Microgravity Science Applications (Code U)
(202) 358-0689 or
rcrouch@hq.nasa.gov

Granville Paules

Office of Mission to Planet Earth (Code Y)
(202) 358-0706 or
gpaules@mtpe.hq.nasa.gov



TECH BRIEFS

NATIONAL AERONAUTICS AND SPACE ADMINISTRATION



5 Technology Focus: Sensors

- 5 Analysis of SSEM Sensor Data Using BEAM
- 5 Hairlike Percutaneous Photochemical Sensors
- 6 Video Guidance Sensors Using Remotely Activated Targets
- 7 Simulating Remote Sensing Systems



9 Electronics/Computers

- 9 EHW Approach to Temperature Compensation of Electronics
- 10 Polymorphic Electronic Circuits
- 11 Micro-Tubular Fuel Cells
- 12 Whispering-Gallery-Mode Tunable Narrow-Band-Pass Filter



15 Software

- 15 PVM Wrapper
- 15 Simulation of Hyperspectral Images
- 15 Algorithm for Controlling a Centrifugal Compressor



17 Mechanics

- 17 Hybrid Inflatable Pressure Vessel
- 18 Double-Acting, Locking Carabiners
- 18 Position Sensor Integral With a Linear Actuator
- 19 Improved Electromagnetic Brake
- 20 Flow Straightener for a Rotating-Drum Liquid Separator



21 Machinery/Automation

- 21 Sensory-Feedback Exoskeletal Arm Controller
- 22 Active Suppression of Instabilities in Engine Combustors



23 Manufacturing

- 23 Fabrication of Robust, Flat, Thinned, UV-Imaging CCDs
- 24 Chemical Thinning Process for Fabricating UV-Imaging CCDs



25 Physical Sciences

- 25 Pseudoslit Spectrometer
- 25 Waste-Heat-Driven Cooling Using Complex Compound Sorbents
- 26 Improved Refractometer for Measuring Temperatures of Drops
- 26 Semiconductor Lasers Containing Quantum Wells in Junctions
- 27 Phytoplankton-Fluorescence-Lifetime Vertical Profiler



29 Information Sciences

- 29 Hexagonal Pixels and Indexing Scheme for Binary Images
- 30 Finding Minimum-Power Broadcast Trees for Wireless Networks
- 31 Automation of Design Engineering Processes

This document was prepared under the sponsorship of the National Aeronautics and Space Administration. Neither the United States Government nor any person acting on behalf of the United States Government assumes any liability resulting from the use of the information contained in this document, or warrants that such use will be free from privately owned rights.

Analysis of SSEM Sensor Data Using BEAM

NASA's Jet Propulsion Laboratory, Pasadena, California

A report describes analysis of space shuttle main engine (SSME) sensor data using Beacon-based Exception Analysis for Multimissions (BEAM) [NASA Tech Briefs articles, the two most relevant being "Beacon-Based Exception Analysis for Multimissions" (NPO-20827), Vol. 26, No.9 (September 2002), page 32 and "Integrated Formulation of Beacon-Based Exception Analysis for Multimissions" (NPO-21126), Vol. 27, No. 3 (March 2003), page 74] for automated detection of anomalies. A specific implementation of BEAM, using the Dynamical Invari-

ant Anomaly Detector (DIAD), is used to find anomalies commonly encountered during SSME ground test firings. The DIAD detects anomalies by computing coefficients of an autoregressive model and comparing them to expected values extracted from previous training data. The DIAD was trained using nominal SSME test-firing data. DIAD detected all the major anomalies including blade failures, frozen sense lines, and deactivated sensors. The DIAD was particularly sensitive to anomalies caused by faulty sensors and unexpected transients. The system of-

fers a way to reduce SSME analysis time and cost by automatically indicating specific time periods, signals, and features contributing to each anomaly. The software described here executes on a standard workstation and delivers analyses in seconds, a computing time comparable to or faster than the test duration itself, offering potential for real-time analysis.

This work was done by Michail Zak, Han Park, and Mark James of Caltech for NASA's Jet Propulsion Laboratory. Further information is contained in a TSP (see page 1). NPO-30664

Hairlike Percutaneous Photochemical Sensors

Mass-produced, inexpensive sensors would be small enough to be minimally invasive.

NASA's Jet Propulsion Laboratory, Pasadena, California

Instrumentation systems based on hairlike fiber-optic photochemical sensors have been proposed as minimally invasive means of detecting biochemicals associated with cancer and other diseases. The fiber-optic sensors could be mass-produced as inexpensive, disposable components. The sensory tip of a fiber-optic sensor would be injected through the patient's skin into subcutaneous tissue. A biosensing material on the sensory tip would bind or otherwise react with the biochemical(s) of interest [the analyte(s)] to produce a change in optical properties that would be measured by use of an external photonic analyzer. After use, a fiber-optic sensor could be simply removed by plucking it out with tweezers.

A fiber-optic sensor according to the proposal would be of the approximate size and shape of a human hair, and its sensory tip would resemble a follicle. Once inserted into a patient's subcutaneous tissue, the sensor would even more closely resemble a hair growing from a follicle (see Figure 1). The biosensing material on the sensory tip could consist of a chemical and/or cells cultured and modified for the purpose. The biosensing material would be con-

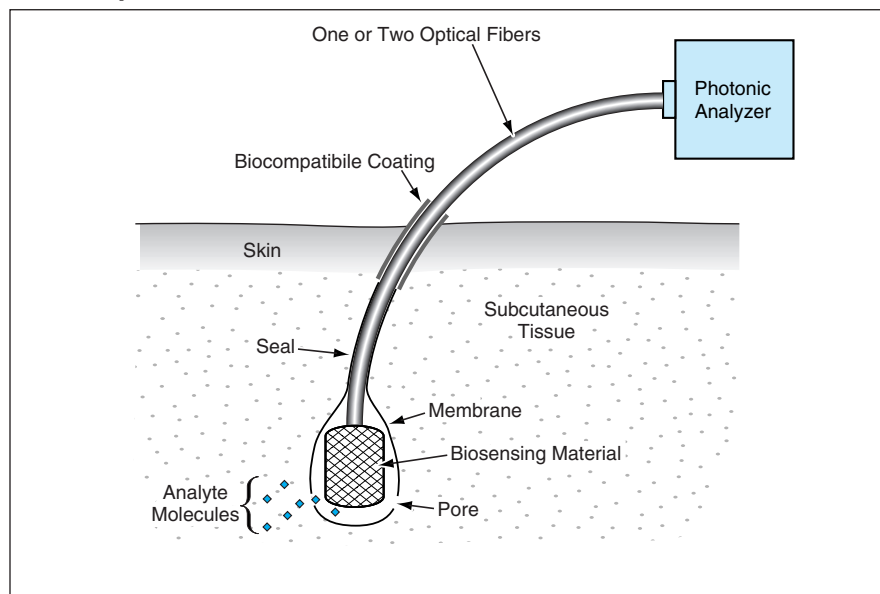


Figure 1. A **Fiber-Optic Sensor** would be implanted through the skin into subcutaneous tissue. The sensory tip would contain a biosensing material that, upon reaction with analyte molecules, would undergo a change in optical properties.

tained within a membrane that would cover the tip. If the membrane were not permeable by an analyte, then it would be necessary to create pores in the membrane that would be large enough to allow analyte molecules to diffuse to the biosensing material, but not so large as

to allow cells (if present as part of the biosensing material) to diffuse out. The end of the fiber-optic sensor opposite the sensory tip would be inserted in a fiber-optic socket in the photonic analyzer.

The basic concept of photonic detection of an analyte admits of the use of

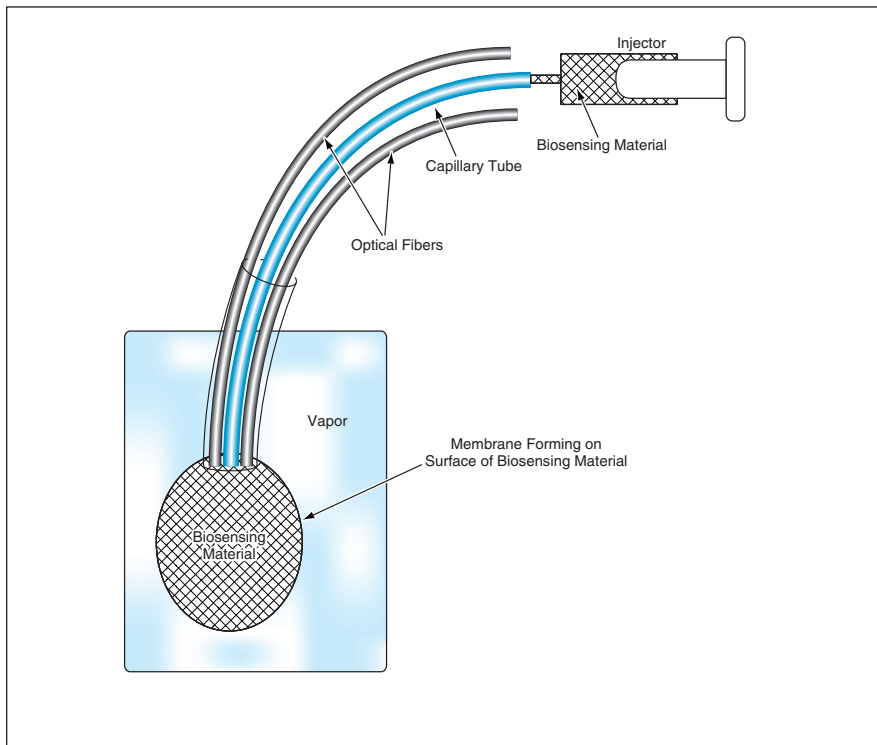


Figure 2. A Fiber-Optic Sensor Could Be Fabricated in a process that would include placement of a droplet containing biosensing material on the tip and vapor deposition of a polymer on the droplet and the optical fibers.

any of several alternative techniques. In one well-known technique, the biosensing material would be illuminated with light having the proper wavelength to excite fluorescence. The intensity and/or wavelength of the fluorescence would depend on the presence or absence of the bound analyte. In some cases, it may be desirable to use the same optical fiber to transmit the exciting light to the sensor and to transmit the fluorescence back to the photonic analyzer. The use of a single fiber would be appropriate if, for example, a brief excitation pulse of light could be expected to produce a longer-lived fluorescence that could be detected after the excitation pulse had been extinguished. In other cases, it may be neces-

sary to use one optical fiber to transmit the excitation light to the biosensing material and another fiber to transmit the fluorescence back to the photonic analyzer. Alternatively or in addition to using fluorescence, it could be possible to measure the concentration of an analyte in terms of the amount of absorption of light of a particular wavelength from a broadband or spectrally modulated illumination.

Figure 2 illustrates a process that might be used to fabricate a two-fiber sensor according to the proposal. The two optical fibers would be bundled with a capillary tube at the end destined to become the sensory tip. The bundled end would be placed in a chamber, which would be partly evacuated and

then back-filled with the vapor of a vapor-depositable material. As the vapor condensed and polymerized on the surface of the bundle, a droplet of biosensing material would be injected through the capillary tube. The droplet would become cooled rapidly by rapid evaporation in the partial vacuum. The cooling of the droplet would increase the rate of condensation of vapor and polymerization on the surface of the droplet, thereby causing the formation of the aforementioned membrane, which would be continuous with a tightly adherent coat over the contiguous optical fibers and capillary tube.

A suitable vapor-depositable material could be Parylene — a thermoplastic polymer made from poly-para-xylylene. Parylene is a highly biocompatible material that tends to discourage the adhesion and tracking of epithelial cells. Because Parylene exhibits little or no permeability by typical analytes that one might seek to detect, it would be necessary to create pores in the membrane. This could be done by, for example, burning holes by use of a tightly focused laser beam.

This work was done by Thomas George of Caltech and Gerald Loeb of the University of Southern California for NASA's Jet Propulsion Laboratory. Further information is contained in a TSP (see page 1).

In accordance with Public Law 96-517, the contractor has elected to retain title to this invention. Inquiries concerning rights for its commercial use should be addressed to:

*Innovative Technology Assets Management
JPL*

*Mail Stop 202-233
4800 Oak Grove Drive
Pasadena, CA 91109-8099
(818) 354-2240*

E-mail: iaoffice@jpl.nasa.gov

Refer to NPO-30651, volume and number of this NASA Tech Briefs issue, and the page number.

Video Guidance Sensors Using Remotely Activated Targets

These systems would not rely on wire connections or GPS signals for synchronization.

Marshall Space Flight Center, Alabama

Four updated video guidance sensor (VGS) systems have been proposed. As described in a previous *NASA Tech Briefs* article, a VGS system is an optoelectronic system that provides guidance for automated docking of two ve-

hicles. The VGS provides relative position and attitude (6-DOF) information between the VGS and its target. In the original intended application, the two vehicles would be spacecraft, but the basic principles of design and opera-

tion of the system are applicable to aircraft, robots, objects maneuvered by cranes, or other objects that may be required to be aligned and brought together automatically or under remote control.

In the first two of the four VGS systems as now proposed, the tracked vehicle would include active targets that would light up on command from the tracking vehicle, and a video camera on the tracking vehicle would be synchronized with, and would acquire images of, the active targets. The video camera would also acquire background images during the periods between target illuminations. The images would be digitized and the background images would be subtracted from the illuminated-target images. Then the position and orientation of the tracked vehicle relative to the tracking vehicle would be computed from the known geometric relationships among the positions of the targets in the image, the positions of the targets relative to each other and to the rest of the tracked vehicle, and the position and orientation of the video camera relative to the rest of the tracking vehicle.

The major difference between the first two proposed systems and prior active-target VGS systems lies in the techniques for synchronizing the flashing of the active targets with the digitization and processing of image data. In the prior active-target VGS systems, synchronization was effected, variously, by use of either a wire connection or the Global Positioning System (GPS). In three of the proposed VGS systems, the synchronizing signal would be generated on, and transmitted from, the tracking vehicle.

In the first proposed VGS system, the tracking vehicle would transmit a pulse of light. Upon reception of the pulse, circuitry on the tracked vehicle would activate the target lights. During the pulse, the target image acquired by the

camera would be digitized. When the pulse was turned off, the target lights would be turned off and the background video image would be digitized.

The second proposed system would function similarly to the first proposed system, except that the transmitted synchronizing signal would be a radio pulse instead of a light pulse. In this system, the signal receptor would be a rectifying antenna. If the signal contained sufficient power, the output of the rectifying antenna could be used to activate the target lights, making it unnecessary to include a battery or other power supply for the targets on the tracked vehicle.

The third proposed VGS system could include either passive or active targets. This system would include two or more video cameras and associated digitizing and digital image-processing circuitry on the tracking vehicle for acquiring stereoscopic pairs of images of the targets on the tracked vehicle. At distances beyond the normal VGS operating range (that is, at distances so great that the target images would merge into a single spot of light on each camera focal plane), a VGS system operating in its normal short-range mode could determine the direction to the tracked vehicle but could not determine the distance to, or the orientation of, the tracked vehicle. However, in such a situation, this proposed system would determine the distance to the tracked vehicle by use of the known geometric relationships of stereoscopy — provided, of course, that the distance were not so great as to bring the stereoscopic disparity below the minimum useful level.

The fourth proposed system would be an active-target VGS system in which synchronization would not involve the transmission of pulses from the tracking vehicle. Instead, the target lights would be flashed at a repetition rate of 5 Hz governed by a free-running oscillator on the tracked vehicle. Each flash period would include a lights-on interval of $3/60$ of a second (corresponding to three video fields at standard video frame rate of 30 Hz at two fields per frame) and a lights-off interval of $9/60$ of second. The system would digitize two pictures in a row, subtract them, and look for the expected target pattern in each synthetic image generated by the subtraction. If the target pattern were thus found, then the flash timing would be known to within one field. If the target pattern were not found, then the time of each picture would be advanced one frame (two fields — $1/30$ of a second) relative to the beginning of a 5-Hz processing cycle and the aforementioned actions repeated. This process would quickly bring the digitizing and data-processing circuitry into synchronism with the flashing of the targets.

This work was done by Thomas C. Bryan, Richard T. Howard, and Michael L. Book of Marshall Space Flight Center. Further information is contained in a TSP (see page 1).

This invention has been patented by NASA (U.S. Patent No. 6,254,035). Inquiries concerning nonexclusive or exclusive license for its commercial development should be addressed to Sammy Nabors, MSFC Commercialization Assistance Lead, at (256) 544-5226 or sammy.nabors@msfc.nasa.gov. Refer to MFS-31278/79/80/81.

Simulating Remote Sensing Systems

Stennis Space Center, Mississippi

The Application Research Toolbox (ART) is a collection of computer programs that implement algorithms and mathematical models for simulating remote sensing systems. The ART is intended to be especially useful for performing design-tradeoff studies and statistical analyses to support the rational development of design requirements for multispectral imaging systems. Among other things, the ART affords a capability to synthesize coarser-spatial-resolution image-data products. The ART also provides for simulations of

image-degradation effects, including point-spread functions, misregistration of spectral images, and noise. The ART can utilize real or synthetic data sets, along with sensor specifications, to create simulated data sets. In one example of a particular application, simulated imagery of a coarse resolution system was created using high-resolution imagery from another system in order to perform a radiometric cross-comparison. In the case of a proposed sensor system, the simulated data can be used to conduct trade studies and statistical analyses

to ensure that the sensor system will satisfy the requirements of potential scientific, academic, and commercial user communities.

This collection of programs was written by Vicki Zaroni of Stennis Space Center and Robert Ryan, Slawomir Blonski, Jeffrey Russell, Gerald Gasser, and Randall Greer of Lockheed Martin Corp.

Inquiries concerning rights for the commercial use of this invention should be addressed to the Intellectual Property Manager, Stennis Space Center, (228) 688-1929. Refer to SSC-00181.



EHW Approach to Temperature Compensation of Electronics

Circuits would be evolved to recover functionality lost in temperature excursions.

NASA's Jet Propulsion Laboratory, Pasadena, California

Efforts are under way to apply the concept of evolvable hardware (EHW) to compensate for variations, with temperature, in the operational characteristics of electronic circuits. To maintain the required functionality of a given circuit at a temperature above or below the nominal operating temperature for which the circuit was originally designed, a new circuit would be evolved; moreover, to obtain the required functionality over a very wide temperature range, there would be evolved a number of circuits, each of which would satisfy the performance requirements over a small part of the total temperature range.

The basic concepts and some specific implementations of EHW were described in a number of previous *NASA Tech Briefs* articles, namely, "Reconfigurable Arrays of Transistors for Evolvable Hardware" (NPO-20078), Vol. 25, No. 2 (February 2001), page 36; "Evolutionary Automated

Synthesis of Electronic Circuits" (NPO-20535), Vol. 26, No. 7 (July 2002), page 37; "Designing Reconfigurable Antennas Through Hardware Evolution" (NPO-20666), Vol. 26, No. 7 (July 2002), page 38; "'Morphing' in Evolutionary Synthesis of Electronic Circuits" (NPO-20837), Vol. 26, No. 8 (August 2002), page 31; "Mixtrinsic Evolutionary Synthesis of Electronic Circuits" (NPO-20773) Vol. 26, No. 8 (August 2002), page 32; and "Synthesis of Fuzzy-Logic Circuits in Evolvable Hardware" (NPO-21095) Vol. 26, No. 11 (November 2002), page 38.

To recapitulate from the cited prior articles: EHW is characterized as evolutionary in a quasi-genetic sense. The essence of EHW is to construct and test a sequence of populations of circuits that function as incrementally better solutions of a given design problem through the selective, repetitive connection and/or dis-

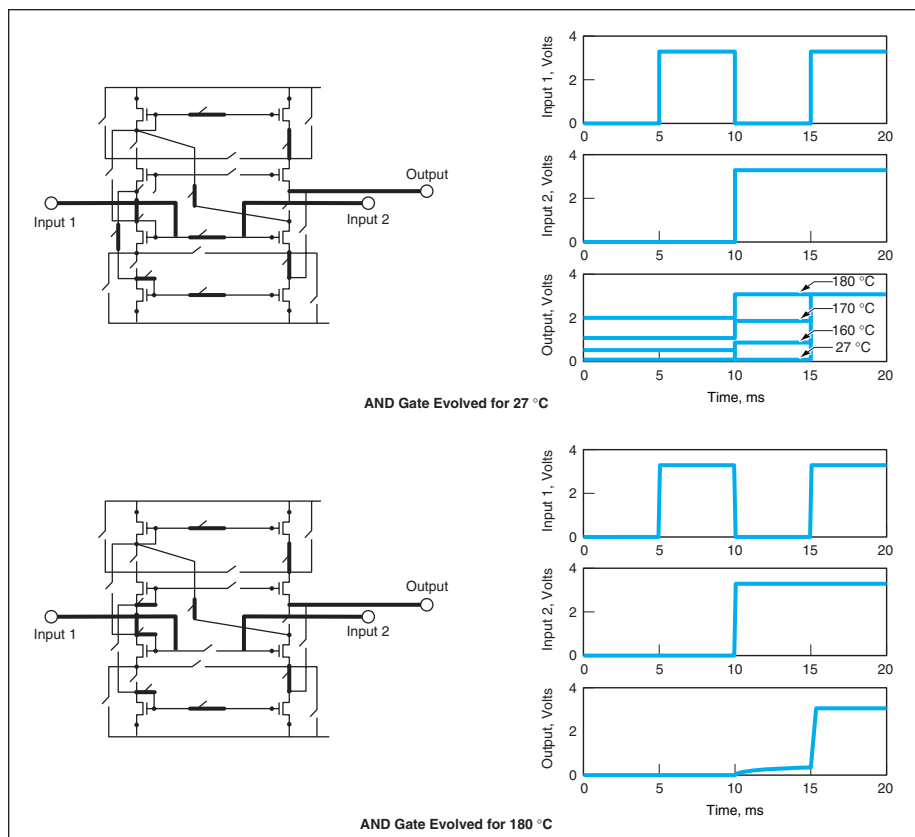
connection of capacitors, transistors, amplifiers, inverters, and/or other circuit building blocks. The connection and disconnection can be effected by use of field-programmable transistor arrays (FPTAs). The evolution is guided by a search-and-optimization algorithm (in particular, a genetic algorithm) that operates in the space of possible circuits to find a circuit that exhibits an acceptably close approximation of the desired functionality. The evolved circuits can be tested by mathematical modeling (that is, computational simulation) only, tested in real hardware, or tested in combinations of computational simulation and real hardware.

In principle, the application of the EHW concept to temperature compensation could be straightforward: If, for example, a change in temperature were to change the functionality of an EHW circuit such as to cause a measure of the

error in the functionality to exceed a specified threshold, then the process of evolutionary automated synthesis could be resumed, possibly taking account of previous circuit configurations in the population. The evolutionary process would be stopped once an evolved circuit performed with an error below the threshold.

The application of the EHW concept to temperature compensation has been demonstrated in computational simulations and in experiments on real FPTAs at controlled temperatures. In one set of computational simulations, an AND gate was evolved to function at a temperature of 27 °C. As shown in the upper part of the figure, its response deteriorated as the temperature was increased to 180 °C. The evolutionary process was then begun toward a new version of the circuit in the hope of restoring the desired AND-gate function at 180 °C. As shown in the lower part of the figure, the evolution yielded a close approximation of the desired result.

This work was done by Adrian Stoica of Caltech for NASA's Jet Propulsion Laboratory. Further information is contained in a TSP (see page 1). NPO-21146



An AND Gate evolved for 27 °C gave a spurious response that increased as temperature was increased to 180 °C. A new AND gate was then evolved for 180 °C.

Polymorphic Electronic Circuits

Circuits are designed to perform different functions under different conditions.

NASA's Jet Propulsion Laboratory, Pasadena, California

Polymorphic electronics is a nascent technological discipline that involves, among other things, designing the same circuit to perform different analog and/or digital functions under different conditions. For example, a circuit can be designed to function as an OR gate or an AND gate, depending on the temperature (see figure). Polymorphic electronics can also be considered a subset of polytronics, which is a broader technological discipline in which optical and possibly other information-processing systems could also be designed to perform multiple functions.

Polytronics is an outgrowth of evolvable hardware (EHW). The basic concepts and some specific implementations of EHW were described in a number of previous *NASA Tech Briefs* articles. To recapitulate: The essence of EHW is to design, construct, and test a sequence of populations of circuits that function as incrementally better solutions of a given design problem through the selective, repetitive connection and/or disconnection of capacitors, transistors, amplifiers, inverters, and/or other circuit building blocks. The evolution is guided by a search-and-optimization algorithm (in particular, a genetic algorithm) that operates in the space of possible circuits

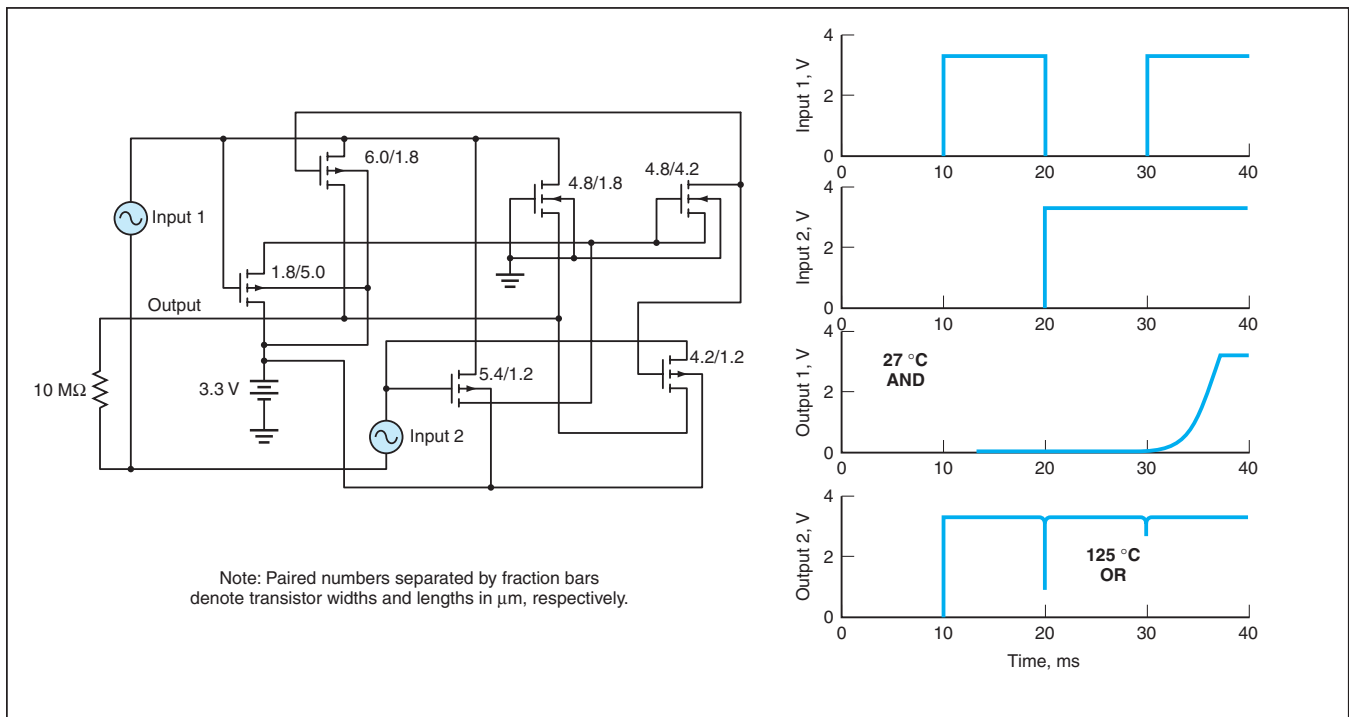
to find a circuit that exhibits an acceptably close approximation of the desired functionality. The evolved circuits can be tested by computational simulation (in which case the evolution is said to be extrinsic), tested in real hardware (in which case the evolution is said to be intrinsic), or tested in random sequences of computational simulation and real hardware (in which case the evolution is said to be mixtrinsic).

The *NASA Tech Briefs* article most relevant to the emergence of polytronics is the preceding article, "EHW Approach to Temperature Compensation of Electronics." Polytronics originated from recognition that the EHW approach makes it possible to go beyond mere compensation for deterioration of circuit functionality with temperature: The EHW approach is a means of designing a circuit to perform an acceptable approximation of almost any desired function at one or more temperatures. In addition to or instead of temperature, the functionality of a circuit could be made to depend on such variables as supply or bias potentials, states of digital control signals, signal frequencies, and/or the intensity of illumination.

Going beyond the temperature-dependent AND/OR gate, the following are a few additional examples of multifunctionality that could be implemented in polytronics:

- A digital circuit could pass data in either of two opposite directions and perform the same function or different functions in the two directions.
- The modes of operation of an entire computer or other complex circuit could be changed almost instantaneously by changing the temperature, supply voltage, or other parameter(s).
- A circuit could be made to perform one (or more) hidden function(s) in addition to a readily observable main function. For example, a hidden function could be an authentication signal that would appear only under specified conditions (for example, supply voltage above a specified level and temperature below a specified level).
- An increase in temperature beyond a specified level could trigger a desired reactive behavior. For example a "smart fuse" circuit could cause guidance circuitry to function differently at higher temperature.

The current research in polytronics involves two modes of evolution that, in EHW,



The Same Circuit Performs as One of Two Logic Gates, depending on the temperature. At 27 °C, it is an AND gate; at 125 °C, it is an OR gate.

would have been denoted as extrinsic and mixtrinsic, respectively. Each mode is characterized by a different combination of advantages and disadvantages.

- In one mode, evolution occurs entirely by computational simulation. For example, circuits can be computationally modeled as consisting only of negative-channel metal oxide semiconductor (NMOS) and positive-channel metal oxide semiconductor (PMOS) transistors that can be connected in arbitrary topologies. The advantage of this mode is that it enables free exploration of the search space, with few or no topological restrictions like those that occur in practice; the lack of restrictions can favor the emergence of new designs. The disadvantage of this approach is that there is no implementation of evolved designs in hardware.

- In the other mode, the circuit topologies are restricted to those of field-programmable transistor arrays (FPTAs). Evolution involves both (1) simulations on computational models of FPTAs and (2) experiments on real FPTAs that are constructed and tested in efforts to implement the models. The advantages of this mode are that circuits can be implemented in practice after evolution, and FPTA chips can be reconfigured to map different polymorphic gates onto them, as needed. The disadvantages of this mode are that (1) the topologies are restricted and (2) in some cases, circuits evolved taking account of the nonideal characteristics (e.g., non-zero "ON" resistances and finite "OFF" resistances of transistor switches) of realistic components can be more complicated than those

evolved through models of ideal components.

This work was done by Adrian Stoica of Caltech for NASA's Jet Propulsion Laboratory. Further information is contained in a TSP (see page 1).

In accordance with Public Law 96-517, the contractor has elected to retain title to this invention. Inquiries concerning rights for its commercial use should be addressed to

Intellectual Assets Office

JPL

Mail Stop 202-233

4800 Oak Grove Drive

Pasadena, CA 91109

(818) 354-2240

E-mail: ipgroup@jpl.nasa.gov

Refer to NPO-21213, volume and number of this NASA Tech Briefs issue, and the page number.

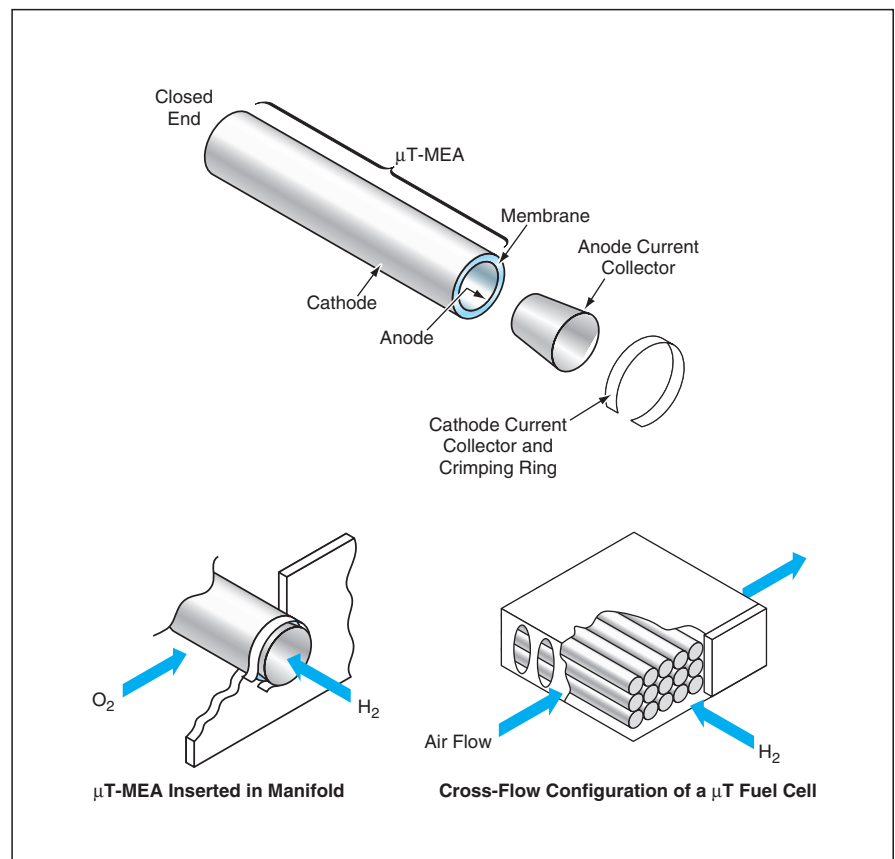
Micro-Tubular Fuel Cells

Power densities would be much greater than those of conventional fuel cells.

Lyndon B. Johnson Space Center, Houston, Texas

Micro-tubular fuel cells that would operate at power levels on the order of hundreds of watts or less are under development as alternatives to batteries in numerous products — portable power tools, cellular telephones, laptop computers, portable television receivers, and small robotic vehicles, to name a few examples. Micro-tubular fuel cells exploit advances in the art of proton-exchange-membrane fuel cells. The main advantage of the micro-tubular fuel cells would be higher power densities: Whereas the mass and volume power densities of low-pressure hydrogen-and-oxygen-fuel plate-and-frame fuel cells designed to operate in the targeted power range are typically less than 0.1 W/g and 0.1 kW/L, micro-tubular fuel cells are expected to reach power densities much greater than 1 W/g and 1 kW/L. Because of their higher power densities, micro-tubular fuel cells would be better for powering portable equipment, and would be better suited to applications in which there are requirements for modularity to simplify maintenance or to facilitate scaling to higher power levels.

The development of PEMFCs has conventionally focused on producing large stacks of cells that operate at typi-



A Micro-Tubular Fuel Cell contains multiple tubular membrane/electrode assemblies that operate in an oxygen/hydrogen cross flow. The hydrogen manifold and the edge-tab electrical current collectors take up much less space than do the bipolar plates of conventional plate-and-frame fuel cells.

cal power levels >5 kW. The usual approach taken to developing lower-power PEMFCs for applications like those listed above has been to simply shrink the basic plate-and-frame configuration to smaller dimensions. A conventional plate-and-frame fuel cell contains a membrane/electrode assembly in the form of a flat membrane with electrodes of the same active area bonded to both faces. In order to provide reactants to both electrodes, bipolar plates that contain flow passages are placed on both electrodes. The mass and volume overhead of the bipolar plates amounts to about 75 percent of the total mass and volume of a fuel-cell stack. Removing these bipolar plates in the micro-tubular fuel cell significantly increases the power density.

A micro-tubular fuel cell contains multiple membrane/electrode assemblies, each comprising a tubular proton-exchange membrane with the anode on the inner surface and the cathode on the outer surface (see figure). Targeted dimensions include an inner membrane diameter of 600 μm , membrane thickness of 50 μm , anode thickness of 25 μm , and cathode thickness of 125 μm . One end of each micro-tubular mem-

brane/electrode assembly ($\mu\text{T-MEA}$) is closed, while the other end is open and connected to a current-collection manifold. At the open end of each $\mu\text{T-MEA}$, a conical anode current collector and diffuser is inserted in the tube, and a cathode current-collector/crimping ring is placed around the outside of the tube. Hydrogen gas diffuses into the interiors of the tubes, while air or oxygen is blown across the outside of the tubes in a cross-flow configuration.

The anode and cathode current collectors are connected by an end-plate assembly (not shown in the figure) in the hydrogen-gas manifold that defines the parallel and serial electrical connections of the $\mu\text{T-MEAs}$. Because each $\mu\text{T-MEA}$ produces a relatively small current, parallel and serial connections can be made at their ends without incurring an unacceptably large amount of ohmic heating. Although the cylindrical geometry causes the current density at the anode in each $\mu\text{T-MEA}$ to exceed that at the cathode, this feature detracts only slightly from cell performance because it is a fundamental property of any PEMFC that the anode polarization loss is much less than the cathode polarization loss at a given current density.

The elimination of the bipolar plates in favor of the much less bulky and massive manifold and current-collector assembly is the single greatest contribution to more efficient utilization of available volume and thus to increased power density. It has been estimated that after further optimization of dimensions, materials, and fabrication processes, it should be possible to make micro-tubular fuel cells with power densities as great as 6.4 W/g and 6.9 kW/L.

This work was done by Michael C. Kimble, Everett B. Anderson, Karen D. Jayne, and Alan S. Woodman of Physical Sciences Inc. for Johnson Space Center. For further information, contact the Johnson Commercial Technology Office at (281) 483-3809.

In accordance with Public Law 96-517, the contractor has elected to retain title to this invention. Inquiries concerning rights for its commercial use should be addressed to

Physical Sciences Inc.

20 New England Business Center

Andover, MA 01810-1077

Telephone No.: (978) 689-0003

Fax No.: (978) 689-3232

Refer to MSC-23012, volume and number of this NASA Tech Briefs issue, and the page number.

Whispering-Gallery-Mode Tunable Narrow-Band-Pass Filter

Characteristics include wide tuning range, short tuning time, and compactness.

NASA's Jet Propulsion Laboratory, Pasadena, California

An experimental tunable, narrow-band-pass electro-optical filter is based on a whispering-gallery resonator. This device is a prototype of tunable filters needed for the further development of reconfigurable networking wavelength-division multiplexers and communication systems that utilize radio-frequency (more specifically, microwave) subcarrier signals on optical carrier signals. The characteristics of whispering-gallery resonators that make them attractive for such applications include high tuning speed, compactness, wide tuning range, low power consumption, and compatibility with single-mode optical fibers. In addition, relative to Fabry-Perot resonators, these devices offer advantages of greater robustness and lower cost.

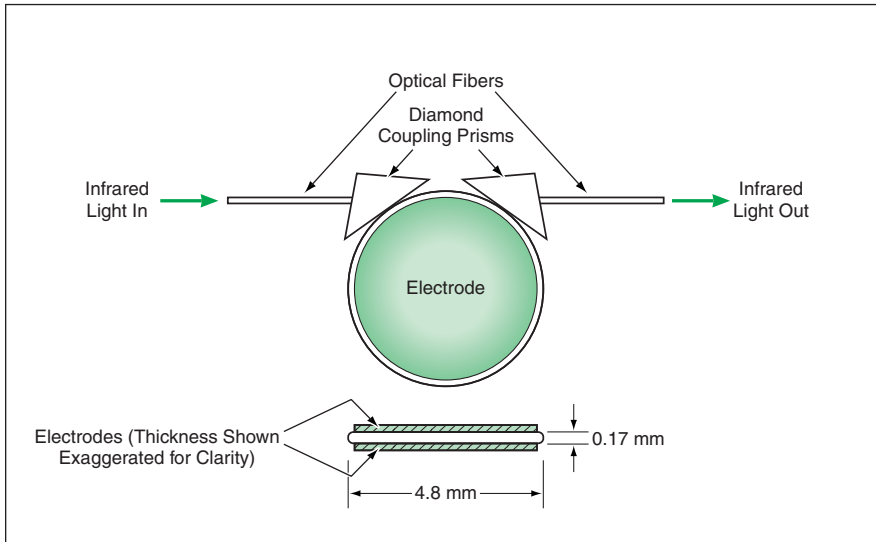
As described in several prior *NASA Tech Briefs* articles, a whispering-gallery resonator is a spheroidal, disklike, or toroidal body made of a highly transparent material. It is so named because it is designed to

exploit whispering-gallery electromagnetic modes, which are waveguide modes that propagate circumferentially and are concentrated in a narrow toroidal region centered on the equatorial plane and located near the outermost edge.

The experimental whispering-gallery tunable filter (see figure) is made from a disk of Z-cut LiNbO_3 of 4.8-mm diameter and 0.17-mm thickness. The perimeter of the disk is rounded to a radius of curvature of 100 μm . Metal coats on the flat faces of the disk serve as electrodes for exploiting the electro-optical effect in LiNbO_3 for tuning. There is no metal coat on the rounded perimeter region, where the whispering-gallery modes propagate. Light is coupled from an input optical fiber into the whispering-gallery modes by means of a diamond prism. Another diamond prism is used to couple light from the whispering-gallery modes to an output optical fiber. This device is designed and operated to

exploit transverse magnetic (TM) whispering-gallery modes, rather than transverse electric (TE) modes because the resonance quality factors (Q values) of the TM modes are higher. If Q values were not of major concern, it would be better to use the TE modes because the electro-optical shifts of the TE modes are 3 times those of the TM modes.

Although this filter has been operated only at wavelengths in the vicinity of 1.55 μm , it is capable of operating at wavelengths from ≈ 1.0 to ≈ 1.7 μm — a range limited only by absorption of light in LiNbO_3 . The free spectral range [FSR (the frequency interval between successive resonances)] of the filter is 10 GHz and the bandwidth is 30 MHz; these figures translate to a finesse of about 300. In contrast, a typical Fabry-Perot filter has a finesse of 100 and a bandwidth of 125 MHz. (The finesse is the ratio between the FSR and the bandwidth. It is commonly used as a figure of merit of a



A **Whispering-Gallery-Mode Resonator** is made from a disk of LiNbO_3 . The whispering-gallery modes are concentrated in the rounded outer edge region. The resonance frequencies are changed by applying a voltage to the electrodes.

Fabry-Perot filter and it approximates the maximum number of communication channels that can fit within one FSR). The filter has been found to be tunable over a frequency range somewhat greater than one FSR, the fre-

quency varying linearly with applied potential at 42 MHz/V over the range of ± 150 V. Although the tuning time of the filter is only 10 ns, the spectrum-shifting time, which is determined by the 30-MHz bandwidth, is ≤ 30 μs . For channels

spaced 50 MHz apart, the filter suppresses cross-talk by about 20 dB.

One disadvantage of this device is an insertion loss of 9 dB. This loss has been attributed primarily to inefficiency of coupling by means of the diamond prisms. It may be possible to reduce the insertion loss by use of antireflection coats on the prisms or special gratings on high-index-of-refraction optical fibers.

This work was done by Anatoliy Savchenkov, Vladimir Itchenko, Andrey Matsko, and Lute Maleki of Caltech for NASA's Jet Propulsion Laboratory. Further information is contained in a TSP (see page 1).

In accordance with Public Law 96-517, the contractor has elected to retain title to this invention. Inquiries concerning rights for its commercial use should be addressed to:

Innovative Technology Assets Management

JPL

Mail Stop 202-233

4800 Oak Grove Drive

Pasadena, CA 91109-8099

(818) 354-2240

E-mail: iaoffice@jpl.nasa.gov

Refer to NPO-30896, volume and number of this NASA Tech Briefs issue, and the page number.

🔗 PVM Wrapper

PVM Wrapper is a software library that makes it possible for code that utilizes the Parallel Virtual Machine (PVM) software library to run using the message-passing interface (MPI) software library, without needing to rewrite the entire code. PVM and MPI are the two most common software libraries used for applications that involve passing of messages among parallel computers. Since about 1996, MPI has been the de facto standard. Codes written when PVM was popular often feature patterns of {"init-send," "pack," "send"} and {"receive," "unpack"} calls. In many cases, these calls are not contiguous and one set of calls may even exist over multiple subroutines. These characteristics make it difficult to obtain equivalent functionality via a single MPI "send" call. Because PVM Wrapper is written to run with MPI-1.2, some PVM functions are not permitted and must be replaced — a task that requires some programming expertise. The "pvm_spawn" and "pvm_parent" function calls are not replaced, but a programmer can use "mpirun" and knowledge of the ranks of parent and child tasks with supplied macroinstructions to enable execution of codes that use "pvm_spawn" and "pvm_parent."

This program was written by Daniel Katz of Caltech for NASA's Jet Propulsion Laboratory. Further information is contained in a TSP (see page 1).

This software is available for commercial licensing. Please contact Don Hart of the California Institute of Technology at (818) 393-3425. Refer to NPO-40232.

🌐 Simulation of Hyperspectral Images

A software package generates simulated hyperspectral imagery for use in validating algorithms that generate estimates of Earth-surface spectral reflectance from hyperspectral images acquired by airborne and spaceborne instruments. This software is based on a direct simulation Monte Carlo approach for modeling three-dimensional atmospheric radiative transport, as well as reflections from surfaces characterized by spatially inhomogeneous bidirectional reflectance distribution functions. In this approach, "ground truth" is accurately known through input specification of surface and atmospheric properties, and it is practical to consider wide variations of these properties. The software can treat both land and ocean surfaces, as well as the effects of finite clouds with surface shadowing. The spectral/spatial data cubes computed by use of this software can serve both as a substitute for, and a supplement to, field validation data.

This program was written by Steven C. Richtsmeier, Alexander Singer-Berk, and Lawrence S. Bernstein of Spectral Sciences, Inc., for Stennis Space Center.

Inquiries concerning rights for the commercial use of this invention should be addressed to the Intellectual Property Manager, Stennis Space Center, (228) 688-1929. Refer to SSC-00183.

⚙️ Algorithm for Controlling a Centrifugal Compressor

An algorithm has been developed for controlling a centrifugal compressor that serves as the prime mover in a heat-pump system. Experimental studies have shown that the operating conditions for maximum compressor efficiency are close to the boundary beyond which surge occurs. Compressor surge is a destructive condition in which there are instantaneous reversals of flow associated with a high outlet-to-inlet pressure differential. For a given cooling load, the algorithm sets the compressor speed at the lowest possible value while adjusting the inlet guide vane angle and diffuser vane angle to maximize efficiency, subject to an overriding requirement to prevent surge. The onset of surge is detected via the onset of oscillations of the electric current supplied to the compressor motor, associated with surge-induced oscillations of the torque exerted by and on the compressor rotor. The algorithm can be implemented in any of several computer languages.

This program was written by Scott M. Benedict of Mainstream Engineering Corp. for Johnson Space Center. For further information, contact:

*Mainstream Engineering Corp.
200 Yellow Place
Rockledge, FL 32955
Telephone No.: (321) 631-3550
www.mainstream-engr.com.
Refer to MSC-23016.*

Hybrid Inflatable Pressure Vessel

A bladder that holds pressure is reinforced with fabric straps.

Lyndon B. Johnson Space Center, Houston, Texas

Figure 1 shows a prototype of a large pressure vessel under development for eventual use as a habitable module for long spaceflight (e.g., for transporting humans to Mars). The vessel is a hybrid that comprises an inflatable shell attached to a rigid central structural core. The inflatable shell is, itself, a hybrid that comprises (1) a pressure bladder restrained against expansion by (2) a web of straps made from high-strength polymeric fabrics. On Earth, pressure vessels like this could be used, for example, as portable habitats that could be set up quickly in remote locations, portable hyperbaric chambers for treatment of decompression sickness, or flotation devices for offshore platforms. In addition, some aspects of the design of the fabric straps could be adapted to such other items as lifting straps, parachute straps, and automotive safety belts.

Figure 2 depicts selected aspects of the design of a vessel of this type with a toroidal configuration. The bladder serves as an impermeable layer to keep air within the pressure vessel and, for this purpose, is sealed to the central structural core. The web includes longitudinal and circumferential straps. To help maintain the proper shape upon inflation after storage, longitudinal and circumferential straps are indexed together



Figure 1. This **Hybrid Inflatable Pressure Vessel** is a lightweight unit that can be stored compactly during transport.

at several of their intersections. Because the web is not required to provide a pressure seal and the bladder is not required to sustain structural loads, the bladder and the web can be optimized for their respective functions. Thus, the bladder can be sealed directly to the rigid core without having to include the web in the seal substructure, and the web can be designed for strength.

The ends of the longitudinal straps are attached to the ends of the rigid structural core by means of clevises. Each clevis pin is surrounded by a roller, around which a longitudinal strap is wrapped to form a lap seam with itself. The roller is of a large diameter chosen to reduce bending of the fibers in the strap. The roller also serves to equalize the load in the portions of the strap on both sides of the clevis pin. The lap seam is formed near the clevis by use of a tapered diamond stitch: This stitch is designed specifically to allow fibers in the stitch and strap to relax under load in such a manner that the load becomes more nearly evenly distributed among all fibers in the stitch region. Thus, the

tapered diamond stitch prevents load concentrations that could cause premature failure of the strap and thereby increases the strength of the strap/structural-core joint. The lap seam can be rated at >90 percent of the strength of the strap material.

The rigid structural core serves partly as an interface for access to the interior of the pressure vessel. The core also serves as a rigid structure for mounting of, and integration with, other equipment to be used in conjunction with the pressure vessel. At each end of the core, there is a pressure bulkhead that can accommodate penetrations for utilities and a hatch for access by personnel. The bulkheads at opposite ends of the core are restrained in their required relative positions by longerons. The core can be completely outfitted with equipment prior to packaging with the inflatable shell. The inflatable shell can be compacted around the rigid structural core for storage and transport and inflated to full size and shape after delivery of the vessel to its destination.

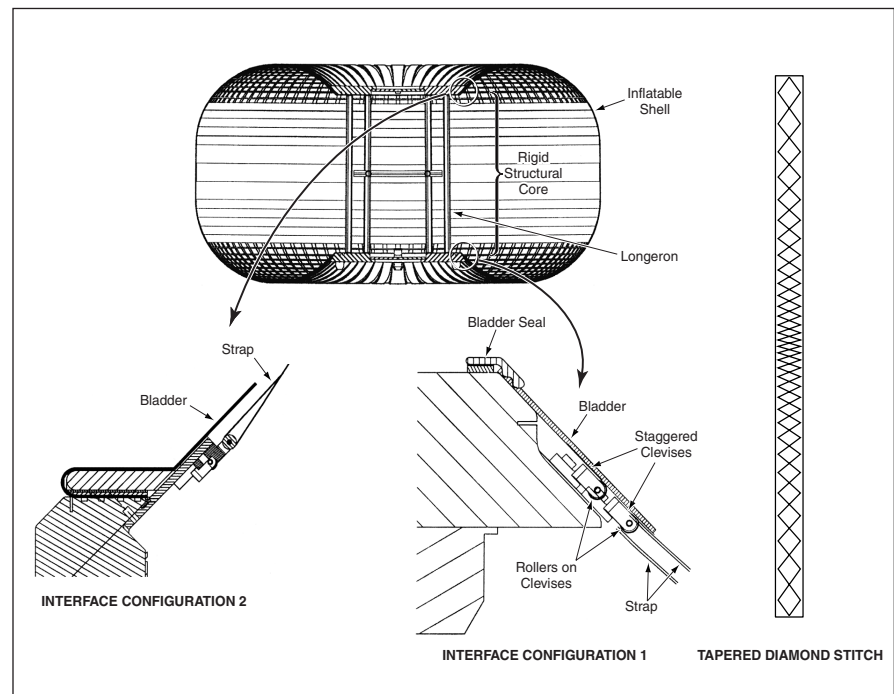


Figure 2. **Several Structural Features** contribute to the effectiveness of the hybrid inflatable pressure vessel.

This work was done by *Jasen L. Raboin, Gerard D. Valle, Gregg Edeen, Horacio M. De La Fuente, William C. Schneider, Gary R. Spexarth, and Christopher J. Johnson* of **Johnson Space Center** and *Shalini Pandya* of

Lockheed Martin. For further information, contact the *Johnson Commercial Technology Office* at (281) 483-3809.

This invention is owned by NASA, and a patent application has been filed. Inquiries

concerning nonexclusive or exclusive license for its commercial development should be addressed to the *Patent Counsel, Johnson Space Center*, (281) 483-0837. Refer to *MSC-23024/92*.

Double-Acting, Locking Carabiners

Lyndon B. Johnson Space Center, Houston, Texas

A proposed design for carabiners (tether hooks used in mountaineering, rock climbing, and rescue) is intended to make it possible to operate these devices even while wearing thick gloves. According to the proposal, the gate of a carabiner would be capable of swinging either toward or away from the hook body, relative to the closed position. The gate would be spring-biased to return to the closed position. An external

locking collar would be pinned to an internal locking rod that would be spring-loaded to slide the collar longitudinally over the gate to lock the gate in the closed position. The gate would be unlocked by sliding the collar axially against the spring load. To reduce the probability of inadvertent unlocking, the rod-and-collar mechanism would include two locking buttons. Option-ally, the rod-and-collar mechanism

could be replaced with an external locking mechanism based on a longer collar.

This work was done by *Chi Min Chang and Dominic Li Del Rosso* of **Johnson Space Center** and *Gary D. Krch* of *ILC Dover*. For further information, contact the *Johnson Commercial Technology Office* at (281) 483-3809. *MSC-23163*

Position Sensor Integral With a Linear Actuator

This sensor adds little to the bulk and weight of the actuator.

Marshall Space Flight Center, Alabama

A noncontact position sensor has been designed for use with a specific two-dimensional linear electromagnetic actuator. To minimize the bulk and weight added by the sensor, the sensor

has been made an integral part of the actuator: that is to say, parts of the actuator structure and circuitry are used for sensing as well as for varying position.

The actuator (see Figure 1) includes a

C-shaped permanent magnet and an armature that is approximately centered in the magnet gap. The intended function of the actuator is to cause the permanent magnet to translate to, and/or remain at, commanded x and y coordinates, relative to the armature. In addition, some incidental relative motion along the z axis is tolerated but not controlled. The sensor is required to measure the x and y displacements from a nominal central position and to be relatively insensitive to z displacement.

The armature contains two sets of electromagnet windings oriented perpendicularly to each other and electrically excited in such a manner as to generate forces in the x,y plane to produce the required motion. Small sensor excitation coils are mounted on the pole tips of the permanent magnet. These coils are excited with a sine wave at a frequency of 20 kHz. This excitation is transformer-coupled to the armature windings. The geometric arrangement of the excitation coils and armature windings is such that the amplitudes of the 20-kHz voltages induced in the armature windings vary nearly linearly with x and y displacements and do not vary significantly with small z displacements. Because the frequency of

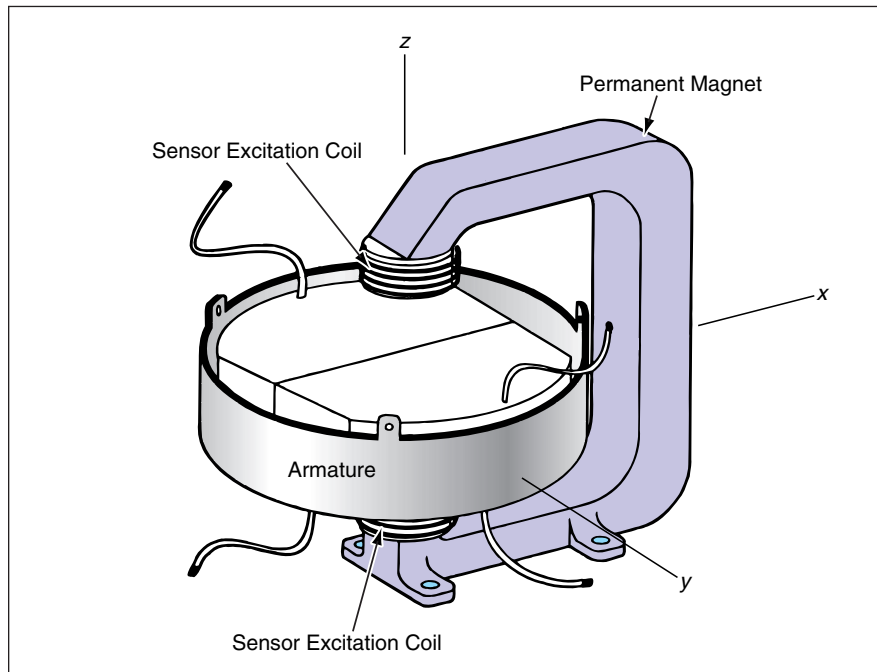


Figure 1. **Sensor Excitation Coils** are the only parts added to the actuator. The electromagnet windings of the actuator are utilized as sensor pickup coils.

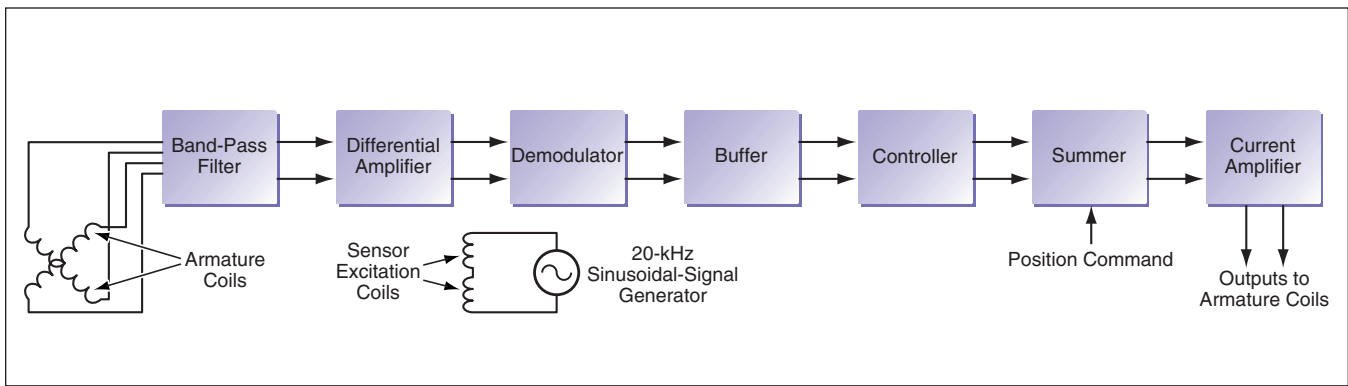


Figure 2. The **Sensor Circuitry** is an **Integral Part** of the actuator position-control circuitry. The actuator displacements in x and y give rise to feedback position-control voltages.

20 kHz is much greater than the maximum frequency characteristic of the actuation signals applied to the armature windings, there is no appreciable interference between actuator and sensor functions of the armature windings.

The voltages across the armature windings are fed as inputs to the circuitry depicted in simplified form in Figure 2. First, the voltages are band-pass filtered at the 20-kHz sensor excitation frequency to minimize lower frequency actuation components and higher-frequency noise com-

ponents. The filtered voltages are processed through a differential amplifier and a demodulator to obtain voltages proportional (in both magnitude and sign) to the x and y displacements. These voltages are fed, through a buffer, as inputs to a proportional + integral + derivative (PID) control circuit. The output of the PID controller is summed with a position-command voltage to obtain a control signal that is fed as input to a current amplifier. The output of the current amplifier, characterized by frequencies much

below 20 kHz, is applied to armature coils to control the x and y displacements.

This work was done by David E. Howard and Dean C. Alhorn of Marshall Space Flight Center.

This invention has been patented by NASA (U.S. Patent No. 6,246,228). Inquiries concerning nonexclusive or exclusive license for its commercial development should be addressed to Sammy Nabors, MSFC Commercialization Assistance Lead, at (256) 544-5226 or sammy.a.nabors@nasa.gov. Refer to MFS-31218.

Improved Electromagnetic Brake

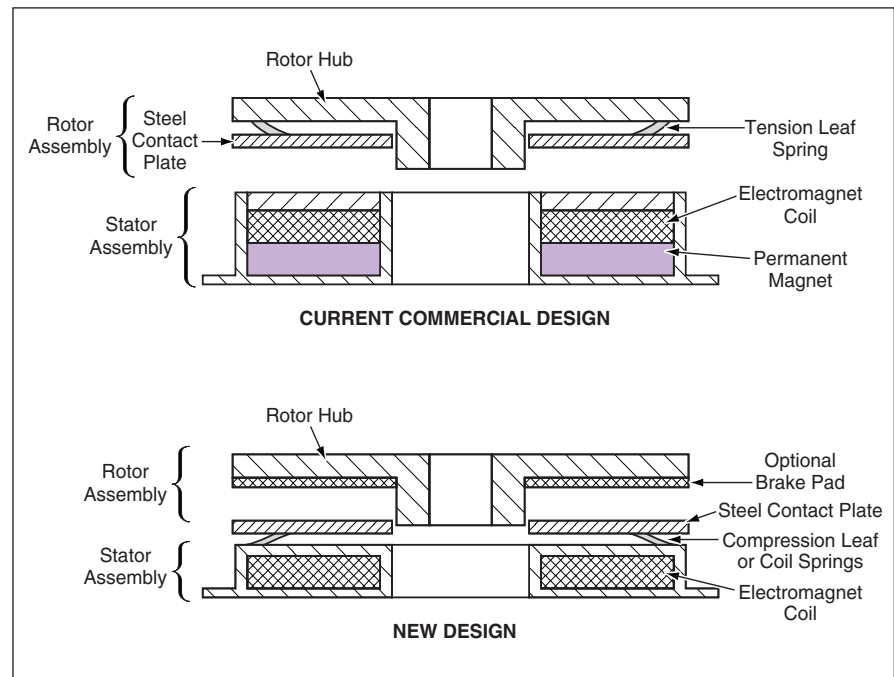
Fail-safe operation would not depend on maintenance of tight tolerances.

Lyndon B. Johnson Space Center, Houston, Texas

A proposed design for an electromagnetic brake would increase the reliability while reducing the number of parts and the weight, relative to a prior commercially available electromagnetic brake. The reductions of weight and the number of parts could also lead to a reduction of cost.

A description of the commercial brake is prerequisite to a description of the proposed electromagnetic brake. The commercial brake (see upper part of figure) includes (1) a permanent magnet and an electromagnet coil on a stator and (2) a rotor that includes a steel contact plate mounted, with tension spring loading, on an aluminum hub. The stator is mounted securely on a stationary object, which would ordinarily be the housing of a gear drive or a motor. The rotor is mounted on the shaft of the gear drive or motor.

The commercial brake nominally operates in a fail-safe (in the sense of normally braking) mode: In the absence of current in the electromagnet coil, the



Current and Proposed Electromagnetic Brakes are depicted here in simplified, partly schematic meridional cross sections.

permanent magnet pulls the contact plate, against the spring tension, into contact with the stator. To release the brake, one excites the electromagnet with a current of the magnitude and polarity chosen to cancel the magnetic flux of the permanent magnet, thereby enabling the spring tension to pull the contact plate out of contact with the stator.

The fail-safe operation of the commercial brake depends on careful mounting of the rotor in relation to the stator. The rotor/stator gap must be set with a tolerance between 10 and 15 mils (between about 0.25 and about 0.38 mm). If the gap or the contact pad is thicker than the maximum allowable value, then the permanent magnetic field will not be strong enough to pull the steel plate across the gap. (For this reason, any contact pad between the contact plate and the stator must also be correspondingly thin.) If the gap exceeds the maximum allowable value because of shaft end play, it becomes impossible to set the brake by

turning off the electromagnet current. Although it may still be possible to set the brake by applying an electromagnet current to aid the permanent magnetic field instead of canceling it, this action can mask an out-of-tolerance condition in the brake and it does not restore the fail-safe function of setting the brake when current is lost.

In the proposed brake (see lower part of figure), the contact pad would be mounted on the stator via compression springs instead of on the rotor via tension springs. Optionally, a steel or ablative brake pad would be mounted on the rotor. There would be no permanent magnet. Instead of using a permanent magnet to pull the contact plate across the rotor/stator gap, one would use the compression springs to push the contact plate into the rotor. An electromagnet would be used to pull the contact plate against the compression springs to release the brake. If the critical gap between the contact plate and the electromagnet were

to grow beyond the reach of the electromagnetic field, the brake could not be released: the contact plate would remain pushed against the rotor — that is, in the braked or fail-safe configuration.

In the proposed design, longitudinal movement of the shaft could be accommodated by increasing the throw of the compression springs. The tolerance on the rotor/stator gap could be increased to as much as tenths of an inch (several millimeters), and the failure mode would change from not being able to set the brake to not being able to release the brake. Also, inasmuch as the frictional braking contact would no longer be between the steel contact plate and the actuating electromagnet, a contact pad of any thickness or material could be mounted on the rotor.

This work was done by Toby B. Martin of Johnson Space Center. For further information, contact the Johnson Commercial Technology office at (281) 483-0837. MSC-23226

Flow Straightener for a Rotating-Drum Liquid Separator

Lyndon B. Johnson Space Center, Houston, Texas

A flow straightener has been incorporated into a rotary liquid separator that originally comprised an inlet tube, a shroud plate, an impeller, an inner drum, an outer drum, a housing, a pitot tube, and a hollow shaft motor. As a consequence of the original geometry of the impeller, shroud, inner drum, and hollow shaft, swirl was created in the airflow inside the hollow shaft during operation. The swirl speed was large enough to cause a significant pressure drop. The flow straightener consists of vanes on the back side of the

shroud plate. These vanes compartmentalize the inside of the inner drum in such a way as to break up the flow path and thereby stop the air from swirling; as a result, the air enters the hollow shaft with a predominantly axial velocity instead of a swirl. Tests of the rotary liquid separator at an airflow rate of 10 ft³/min (0.0047 m³/s) revealed that the dynamic pressure drop was 8 in. of water (\approx 2 kPa) in the absence of the flow straightener and was reduced to 1 in. of water (\approx 0.25 kPa) in the presence of the flow straightener.

*This work was done by James R. O'Coin, David G. Converse, and Donald W. Rethke of Hamilton Sundstrand Space Systems International, Inc., for Johnson Space Center. For further information, contact Kristen M. Balukonis, Contract Administrator
Hamilton Sundstrand Space System International, Inc.
One Hamilton Road
Windsor Locks, CT 06096-1010
Telephone No.: (860) 654-6000
MSC-23149*



Sensory-Feedback Exoskeletal Arm Controller

Forces and torques are reflected from a robotic manipulator back to the human wearer.

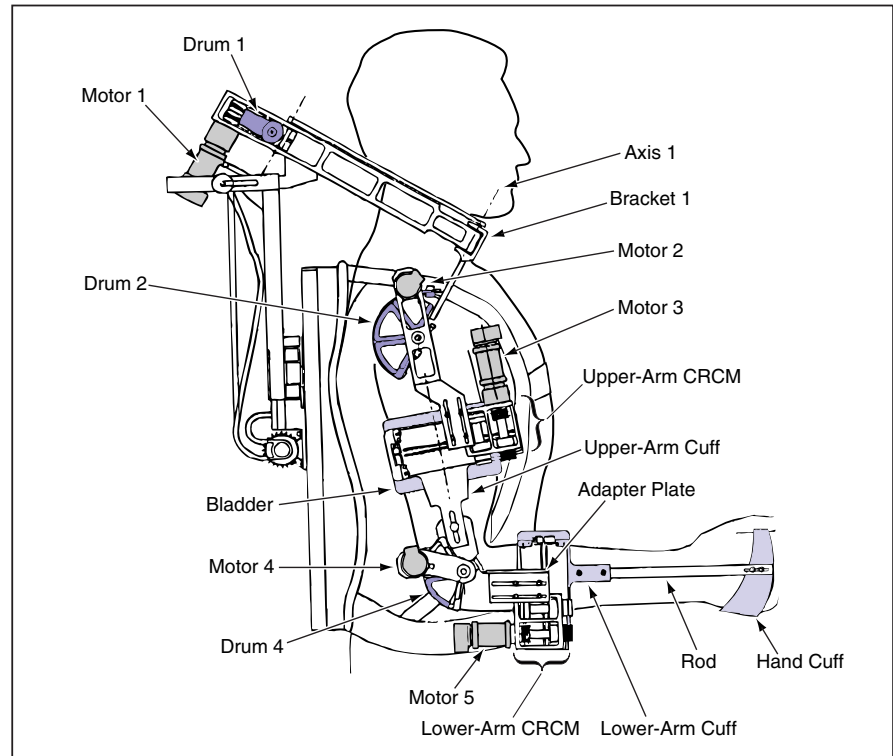
Lyndon B. Johnson Space Center, Houston, Texas

An electromechanical exoskeletal arm apparatus has been designed for use in controlling a remote robotic manipulator arm. The apparatus, called a "force-feedback exoskeleton arm master" (F-EAM) is comfortable to wear and easy to don and doff. It provides control signals from the wearer's arm to a robot arm or a computer simulator (e.g., a virtual-reality system); it also provides force and torque feedback from sensors on the robot arm or from the computer simulator to the wearer's arm. The F-EAM enables the wearer to make the robot arm gently touch objects and finely manipulate them without exerting excessive forces.

The F-EAM features a lightweight design in which the motors and gear heads that generate force and torque feedback are made smaller than they ordinarily would be: this is achieved by driving the motors to power levels greater than would ordinarily be used in order to obtain higher torques, and by providing active liquid cooling of the motors to prevent overheating at the high drive levels.

The F-EAM (see figure) includes an assembly that resembles a backpack and is worn like a backpack, plus an exoskeletal arm mechanism. The F-EAM has five degrees of freedom (DOFs) that correspond to those of the human arm:

1. The first DOF is that of the side-to-side rotation of the upper arm about the shoulder (rotation about axis 1). The reflected torque for this DOF is provided by motor 1 via drum 1 and a planar four-bar linkage.
2. The second DOF is that of the up-and-down rotation of the arm about the shoulder. The reflected torque for this DOF is provided by motor 2 via drum 2.
3. The third DOF is that of twisting of the upper arm about its longitudinal axis. This DOF is implemented in a cable remote-center mechanism (CRCM). The reflected torque for this DOF is provided by motor 3, which drives the upper-arm cuff and the mechanism below it. A bladder inflatable by gas or liquid is placed be-



The Force-Feedback Exoskeleton Arm Master is designed for maximum comfort and low weight to minimize wearer fatigue. Its mechanism imitates the kinematics of the human arm.

4. The fourth DOF is that of flexion and extension of the elbow. The reflected torque for this DOF is provided by motor 4 and drum 4, which are mounted on a bracket that can slide longitudinally by a pin-and-slot engagement with the upper-arm cuff to compensate for slight variations in the position of the kinematic center of the elbow. Attached to drum 4 is an adapter plate to which is attached a CRCM for the lower arm.
5. The lower-arm CRCM implements the fifth DOF, which is the twist of the forearm about its longitudinal axis. Motor 5 provides the reflected torque for this DOF by driving the lower-arm cuff. A rod transmits twist and torsion between the lower-arm cuff and the hand cuff.

With this system, the motion of the wearer's joints and the reflected torques applied to these joints can be measured and controlled in a relatively simple manner. This is because the anthropomorphic design of the mechanism imitates the kinematics of the human arm, eliminating the need for kinematic conversion of joint-torque and joint-angle data.

This work was done by Bin An, Thomas H. Massie, and Vladimir Vayner of Exos, Inc., for Johnson Space Center.

In accordance with Public Law 96-517, the contractor has elected to retain title to this invention. Inquiries concerning rights for its commercial use should be addressed to

*Mr. Bin An
Exos, Inc.
2A Gill St.
Woburn, MA 01801
(617) 933-0022*

Refer to MSC-22563, volume and number of this NASA Tech Briefs issue, and the page number.

Active Suppression of Instabilities in Engine Combustors

Fuel flow would be modulated to generate pressure fluctuations opposing those of instabilities.

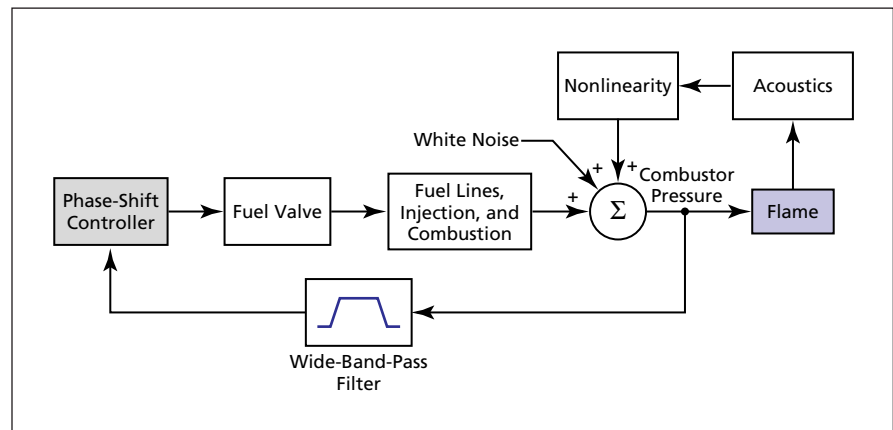
John H. Glenn Research Center, Cleveland, Ohio

A method of feedback control has been proposed as a means of suppressing thermo-acoustic instabilities in a liquid-fueled combustor of a type used in an aircraft engine. The basic principle of the method is one of (1) sensing combustor pressure oscillations associated with instabilities and (2) modulating the rate of flow of fuel to the combustor with a control phase that is chosen adaptively so that the pressure oscillations caused by the modulation oppose the sensed pressure oscillations.

The need for this method arises because of the planned introduction of advanced, lean-burning aircraft gas turbine engines, which promise to operate with higher efficiencies and to emit smaller quantities of nitrogen oxides, relative to those of present aircraft engines. Unfortunately, the advanced engines are more susceptible to thermo-acoustic instabilities. These instabilities are hard to control because they include large dead-time phase shifts, wide-band noise characterized by amplitudes that are large relative to those of the instabilities, exponential growth of the instabilities, random net phase walks, and amplitude fluctuations.

In this method (see figure), the output of a combustion-pressure sensor would be wide-band-pass filtered and then further processed to generate a control signal that would be applied to a fast-actuation valve to modulate the flow of fuel. Initially, the controller would rapidly take large phase steps in order to home in, within a fraction of a second, to a favorable phase region within which the instability would be reduced. Then the controller would restrict itself to operate within this phase region and would further restrict itself to operate within a region of stability, as long as the power in the instability signal was decreasing.

In the phase-shifting scheme of this



This Block Diagram represents a mathematical model of combustion instability and a control system that would suppress the instability by the method described in the main text.

method, the phase of the control vector would be made to continuously bounce back and forth from one boundary of an effective stability region to the other. Computationally, this scheme would be implemented by the adaptive sliding phaser averaged control (ASPAC) algorithm, which requires very little detailed knowledge of the combustor dynamics. In the ASPAC algorithm, the power of the instability signal would be calculated from the wide-band-pass-filtered combustion-pressure signal and averaged over a period of time (typically of the order of a few hundredths of a second) corresponding to the controller updating cycle [not to be confused with the controller sampling cycle, which would be much shorter (typically of the order of 10^{-4} second)]. If the power were found to be decreasing, the direction of change in control phase would be maintained. If the power were found to be increasing, the direction of change of the control phase would be reversed.

A large portion of the algorithm is devoted to quickly recognizing loss of control (equivalently, growth of instability) and re-establishing control within a region of stability before the instability at-

tains an unacceptably large amplitude. The algorithm also includes provisions for discontinuous exponential gain modulation and adaptation of control parameters to further reduce the instability.

In a computational simulation, this method was demonstrated to be effective in reducing instability, characterized by a frequency of about 550 Hz, in an aircraft-engine-type combustor. In addition, in two separate tests conducted during 2002 this control algorithm has been shown to be effective in reducing the instability in the combustor rig, which has many of the complexities of an actual aircraft engine combustor (NASA TM-2003-212535, "High Frequency Adaptive Instability Suppression Controls in a Liquid-Fueled Combustor" report. For information about the report, contact cto@grc.nasa.gov.)

This work was done by George Kopasakis of Glenn Research Center. Further information is contained in a TSP (see page 1).

Inquiries concerning rights for the commercial use of this invention should be addressed to NASA Glenn Research Center, Commercial Technology Office, Attn: Steve Fedor, Mail Stop 4-8, 21000 Brookpark Road, Cleveland Ohio 44135. Refer to LEW-17460.

Fabrication of Robust, Flat, Thinned, UV-Imaging CCDs

Front-side silicon substrates ensure flatness and provide strength.

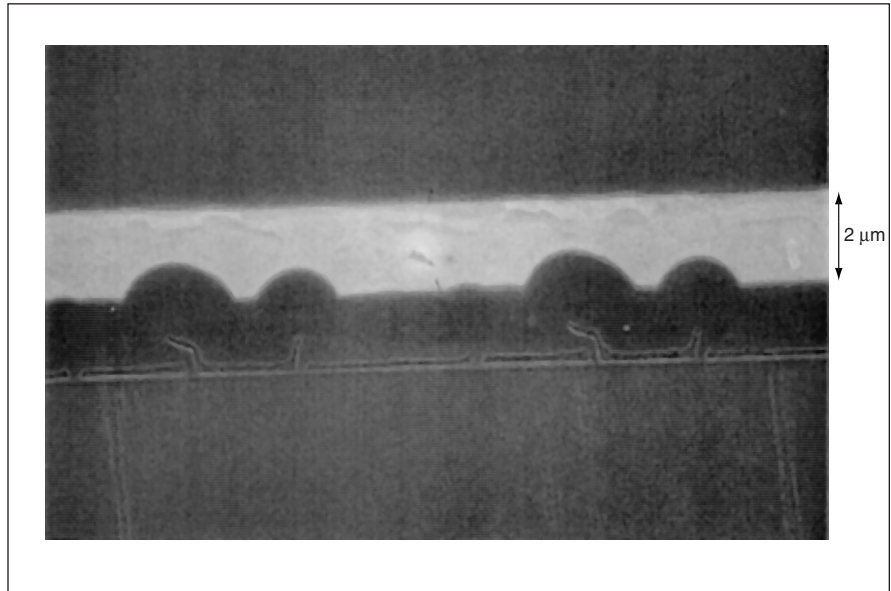
NASA's Jet Propulsion Laboratory, Pasadena, California

An improved process that includes a high-temperature bonding subprocess has been developed to enable the fabrication of robust, flat, silicon-based charge-coupled devices (CCDs) for imaging in ultraviolet (UV) light and/or for detecting low-energy charged particles. The CCDs in question are devices on which CCD circuitry has already been formed and have been thinned for back-surface illumination. These CCDs may be delta doped, and aspects of this type of CCD have been described in several prior articles in *NASA Tech Briefs*. Unlike prior low-temperature bonding subprocesses based on the use of epoxies or waxes, the high-temperature bonding subprocess is compatible with the delta-doping process as well as with other CCD-fabrication processes.

The present improved process and its bonding, thinning, and delta-doping subprocesses, are characterized as post-fabrication processes because they are undertaken after the fabrication of CCD circuitry on the front side of a full-thickness silicon substrate. In a typical case, it is necessary to reduce the thickness of the CCD to between 10 and 20 μm in order to take advantage of back-side illumination and in order to perform delta doping and/or other back-side treatment to enhance the quantum efficiency.

In the prior approach to the fabrication of back-side-illuminated CCDs, the thinning subprocess turned each CCD into a free-standing membrane that was fragile and tended to become wrinkled. In the present improved process, prior to thinning and delta doping, a CCD is bonded on its front side to a silicon substrate that has been prefabricated to include cutouts to accommodate subsequent electrical connections to bonding pads on the CCD circuitry. The substrate provides structural support to increase ruggedness and maintain flatness.

At the beginning of this process, the back side of a CCD as fabricated on a full-thickness substrate is polished. Silicon nitride is deposited on the back side, opposite the bonding pads on the



This **Scanning Electron Micrograph** depicts a cross section of the bond between a CCD and a silicon substrate. The bond is approximately 2 μm thick.

front side, in order to define a relatively thick frame. The portion of the CCD not covered by the frame is the portion to be thinned by etching.

Trilayers of titanium, platinum, and gold are deposited by evaporation on the front side of the CCD and on the mating surface of the matched silicon substrate, in preparation for joining the CCD to the substrate by gold-gold thermocompression bonding. The platinum layers act as barriers to the diffusion of gold into the CCD (necessary because contamination by gold would degrade the performance of the CCD). The titanium layer increases the adhesion of the platinum layer to a protective oxide layer on the CCD. The gold layers on the CCD and the substrate are 1 μm thick. Thermocompression bonding of the CCD and the silicon substrate is performed by heating the assembly to a temperature of 400 $^{\circ}\text{C}$ in a vacuum at a clamping pressure of 10 MPa for 30 minutes. The total gold thickness of 2 μm is sufficient to fill the empty spaces between the CCD pixels and the silicon substrate (see figure).

The CCD-and-substrate unit is placed

back-side up in a fixture, wherein etching by a hot aqueous solution of KOH is performed to reduce the CCD thickness. After etching, the unit is cleaned, then transferred to another fixture that is placed in the ultra-high-vacuum chamber of a molecular-beam-epitaxy apparatus, wherein the delta doping is performed. Finally, the CCD is packaged and wire bonded.

This work was done by Paula Grunthaler, Stythe Elliott, Todd Jones, and Shouleh Nikzad of Caltech for NASA's Jet Propulsion Laboratory. Further information is contained in a TSP (see page 1).

In accordance with Public Law 96-517, the contractor has elected to retain title to this invention. Inquiries concerning rights for its commercial use should be addressed to

Intellectual Assets Office

JPL

Mail Stop 202-233

4800 Oak Grove Drive

Pasadena, CA 91109

(818) 354-2240

E-mail: ipggroup@jpl.nasa.gov

Refer to NPO-30579, volume and number of this NASA Tech Briefs issue, and the page number.

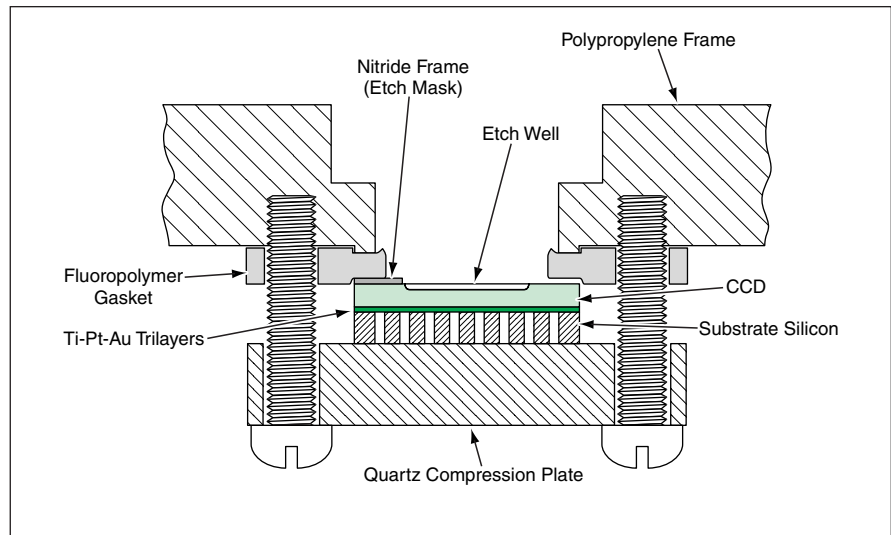
Chemical Thinning Process for Fabricating UV-Imaging CCDs

This process can be used in making CCDs that exhibit high quantum efficiencies.

NASA's Jet Propulsion Laboratory, Pasadena, California

The thinning stage of the postfabrication process reported in the immediately preceding article is notable in its own right. Although the thinning process was described in the preceding article as part of an overall process of fabrication of a supported charge-coupled device (CCD), it is more generally applicable to both free-standing and supported devices that have been fabricated in die and wafer formats. Like the thermocompression bonding process described in the preceding article, the thinning process is compatible with CCD-fabrication processes, as well as postfabrication processes that enhance the response of CCDs to ultraviolet (UV) light, including the delta-doping process. CCDs that are thinned by this process and then delta-doped exhibit high quantum efficiencies that are stable with time and with exposure to the environment.

Once the CCD and substrate have been joined by the thermocompression bonding, the CCD/substrate unit is placed in a fixture with the back side of the CCD die or wafer (the side to be etched) facing up, as shown in the figure. KOH has been chosen as the etchant because it preserves the mirror-smooth finish previously imparted to the CCD wafer or die back surface by chemical mechanical polishing. During etching, a quartz refluxer is used to maintain the concentration of KOH at 55 percent by weight and the solution is stirred continuously and maintained at a temperature of $\approx 80^\circ\text{C}$. The etch rate is between 0.5 and 1.0 $\mu\text{m}/\text{min}$, the exact rate depending on the exact temperature of the solution. Gaskets, along with other parts of the fixture not shown in the figure, seal the die or wafer in the fixture to protect the front-side CCD circuitry against exposure to KOH.



A CCD Bonded to a Silicon Substrate via trilayers of Ti, Pt, and Au is held in a fixture with its back side up for chemical etching to reduce its thickness.

At several intervals during the KOH etch, the fixture is removed from the KOH solution, rinsed, and dried in order to measure the depth of the etch. The etching times are calculated to bring the depth of the etched well to within 20 μm of the epilayer of the CCD device. Removal of the last 20 μm of silicon leading to the epilayer is made by use of a mixture of hydrofluoric, nitric, and acetic acids, which is highly selective: this mixture etches the p^+ bulk silicon at a rate of $\approx 1.5 \mu\text{m}/\text{min}$, and the etch rate falls nearly two orders of magnitude once the p^- epilayer is encountered. Hence, the mixture can be used to remove the remaining p^+ layer. This etch is closely monitored for arrival at the epilayer as indicated by a change in the color, pattern, and intensity of the activity at the solid/liquid interface. Once this etch has been completed, there is a 60-second exposure to another mixture comprising different proportions of the three acids to remove a char-

acteristic dark haze left by etching with the first mixture of the acids. The final etching step is a 90-second exposure to KMnO_4 hydrofluoric acid solution to remove a faint white haze left by the second acid mixture.

This work was done by Todd Jones, Paula Grunthaler, Shouleh Nikzad, and Rick Wilson of Caltech for NASA's Jet Propulsion Laboratory. Further information is contained in a TSP (see page 1).

In accordance with Public Law 96-517, the contractor has elected to retain title to this invention. Inquiries concerning rights for its commercial use should be addressed to

Intellectual Assets Office

JPL

Mail Stop 202-233

4800 Oak Grove Drive

Pasadena, CA 91109

(818) 354-2240

E-mail: ipgroupp@jpl.nasa.gov

Refer to NPO-30578, volume and number of this NASA Tech Briefs issue, and the page number.



Pseudoslit Spectrometer

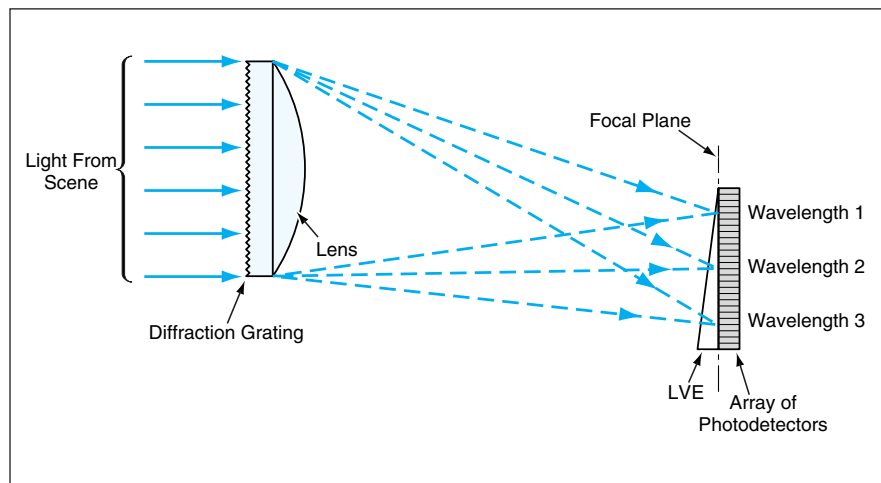
Functioning similarly to a slit spectrometer, this instrument would be optomechanically simpler.

Goddard Space Flight Center, Greenbelt, Maryland

The pseudoslit spectrometer is a conceptual optoelectronic instrument that would offer some of the advantages, without the disadvantages, of prior linear-variable etalon (LVE) spectrometers and prior slit spectrometers. The pseudoslit spectrometer is so named because it would not include a slit, but the combined effects of its optical components would include a spatial filtering effect approximately equivalent to that of a slit.

Like a prior LVE spectrometer, the pseudoslit spectrometer would include an LVE (essentially, a wedgelike narrow-band-pass filter, the pass wavelength of which varies linearly with position in one dimension) in a focal plane covering an imaging planar array of photodetectors. However, the pseudoslit spectrometer would be more efficient because unlike a prior LVE spectrometer, the pseudoslit spectrometer would not have to be scanned across an entire field of view to obtain the spectrum of an object of interest that may occupy only a small portion of the field of view. Like a prior slit spectrometer, the pseudoslit spectrometer could acquire the entire spectrum of such a small object without need for scanning. However, the pseudoslit spectrometer would be optically and mechanically simpler: it would have fewer components and, hence, would pose less of a problem of alignment of components and would be less vulnerable to misalignment.

The pseudoslit spectrometer would include an input optical component



The LVE Would Be Matched, spatially and spectrally, to the focal-plane spectral dispersion pattern of the diffraction grating.

that would both spectrally disperse the light from the scene under observation and focus the light onto the array of photodetectors. The input optical element could be, for example, concave diffraction grating, a combination of a lens and a prism, or, as shown in the figure, a combination of a lens and a diffraction grating. The LVE would be custom fabricated so that, at the focal plane, its spatial variation of pass wavelength would match the spectral dispersion pattern created by the grating. As a result of this match, the LVE would select the spectrum of only one slitlike strip in the field of view.

Hence, position along one axis of the array (in the case of the figure, the axis perpendicular to the page) would corre-

spond to position along the strip in the scene, whereas position along the other axis (the vertical axis in the figure) would correspond to the wavelength of light. In other words, the pseudoslit spectrometer would measure the spectrum of a narrow strip in the scene. To acquire data to construct a spectral image of the entire scene, one would have to scan the pseudoslit spectrometer to scan the strip across the scene.

This work was done by Dennis C. Reuter and George H. McCabe of Goddard Space Flight Center. Further information is contained in a TSP (see page 1). GSC-13806

Waste-Heat-Driven Cooling Using Complex Compound Sorbents

Development of improved sorbents revives a long-neglected heat-pump concept.

Lyndon B. Johnson Space Center, Houston, Texas

Improved complex-compound sorption pumps are undergoing development for use as prime movers in heat-pump systems for cooling and dehumidification of habitats for humans on the Moon and for residential and commercial cooling on Earth. Among the advantages of sorption

heat-pump systems are that they contain no moving parts except for check valves and they can be driven by heat from diverse sources: examples include waste heat from generation of electric power, solar heat, or heat from combustion of natural gas.

The use of complex compound sorbents in cooling cycles is not new in itself: Marketing of residential refrigerators using SrCl₂ was attempted in the 1920s and '30s and was abandoned because heat- and mass-transfer rates of the sorbents were too low. Addressing

the issue that gave rise to the prior abandonment of complex compound sorption heat pumps, the primary accomplishment of the present development program thus far has been the characterization of many candidate sorption media, leading to large increases in achievable heat- and mass-transfer rates. In particular, two complex compounds (called "CC260-1260" and "CC260-2000") were found to be capable of functioning over the temperature range of interest for the lunar-habitat applica-

tion and to offer heat- and mass-transfer rates and a temperature-lift capability adequate for that application.

Regarding the temperature range: A heat pump based on either of these compounds is capable of providing a 95-K lift from a habitable temperature to a heat-rejection (radiator) temperature when driven by waste heat at an input temperature ≥ 500 K. Regarding the heat- and mass-transfer rates or, more precisely, the power densities made possible by these rates: Power densities ob-

served in tests were 0.3 kilowatt of cooling per kilogram of sorbent and 2 kilowatts of heating per kilogram of sorbent. A prototype 1-kilowatt heat pump based on CC260-2000 has been built and demonstrated to function successfully.

This work was done by Uwe Rockefeller, Lance Kirol, and Kaveh Khalili of Rocky Research for Johnson Space Center. For further information, contact the Johnson Commercial Technology Office at (281) 483-3809. MSC-22952

Improved Refractometer for Measuring Temperatures of Drops

The task of upgrading PDPA hardware for measurement of temperature is simplified.

Marshall Space Flight Center, Alabama

The Dual Rainbow refractometer is an enhanced version of the Rainbow refractometer, which is added to, and extends the capabilities of, a phase Doppler particle analyzer (PDPA). A PDPA utilizes pairs of laser beams to measure individual components of velocity and sizes of drops in a spray. The Rainbow-refractometer addition measures the temperatures of individual drops. The designs of prior versions of the Rainbow refractometer have required substantial modifications of PDPA transmitting optics, plus dedicated lasers as sources of illumination separate from, and in addition to, those needed for PDPA measurements. The enhancement embodied in the Dual Rainbow refractometer eliminates the need for a dedicated laser and confers other advantages as described below.

A dedicated laser is no longer needed

because the Dual Rainbow refractometer utilizes one of the pairs of laser beams already present in a PDPA. Hence, the design of the Dual Rainbow refractometer simplifies the task of upgrading PDPA hardware to enable measurement of temperature. Furthermore, in a PDPA/Dual-Rainbow-refractometer system, a single argon-ion laser with three main wavelengths can be used to measure the temperatures, sizes, and all three components of velocity (in contradistinction to only two components of velocity in a prior PDPA/Rainbow-refractometer system).

In order to enable the Dual Rainbow refractometer to utilize a pair of PDPA laser beams, it was necessary to (1) find a location for the refractometer receiver, such that the combined rainbow patterns of two laser beams amount to a pattern identical to that of a single beam, (2) ad-

just the polarization of the two beams to obtain the strongest rainbow pattern, and (3) find a location for the PDPA receiver to obtain a linear relationship between the measured phase shift and drop size.

This work was done by Amir A. Naqwi of Aerometrics/TSI, Inc. for Marshall Space Flight Center. For further information, contact the Company at (651) 490-3836.

In accordance with Public Law 96-517, the contractor has elected to retain title to this invention. Inquiries concerning rights for its commercial use should be addressed to

Aerometrics/TSI, Inc.

Laser Diagnostic Division

500 Cardigan Road

Shoreview, MN 55126

Refer to MFS-31531, volume and number of this NASA Tech Briefs issue, and the page number.

Semiconductor Lasers Containing Quantum Wells in Junctions

Additional design degrees of freedom are available for improving performance.

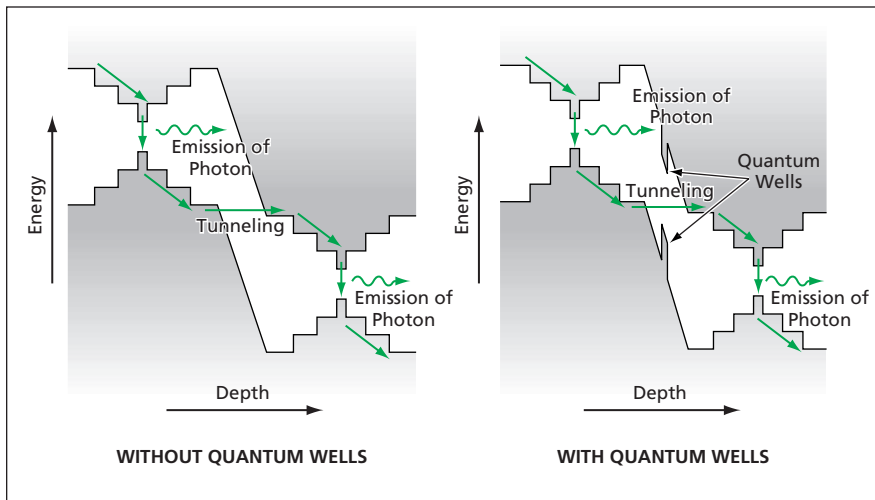
NASA's Jet Propulsion Laboratory, Pasadena, California

In a recent improvement upon $\text{In}_x\text{Ga}_{1-x}\text{As}/\text{InP}$ semiconductor lasers of the bipolar cascade type, quantum wells are added to Esaki tunnel junctions, which are standard parts of such lasers. The energy depths and the geometric locations and thicknesses of the wells are tailored to exploit quantum tunneling such that, as described below, electrical resistances of junctions and concentrations of dopants can be reduced while laser performances can be improved.

$\text{In}_x\text{Ga}_{1-x}\text{As}/\text{InP}$ bipolar cascade lasers have been investigated as sources of near-infrared radiation (specifically, at wavelengths of about 980 and 1,550 nm) for photonic communication systems. The Esaki tunnel junctions in these lasers have been used to connect adjacent cascade stages and to enable transport of charge carriers between them. Typically, large concentrations of both n (electron-donor) and p (electron-ac-

ceptor) dopants have been necessary to impart low electrical resistances to Esaki tunnel junctions. Unfortunately, high doping contributes free-carrier absorption, thereby contributing to optical loss and thereby, further, degrading laser performance.

In accordance with the present innovation, quantum wells are incorporated into the Esaki tunnel junctions so that the effective heights of barriers to quantum tunneling are reduced (see figure).



These Schematic Energy-Band Profiles are typical of a bipolar cascade laser.

Inasmuch as the tunneling current is approximately inversely proportional to the exponential of the barrier height, the introduction of quantum wells into the Esaki tunnel junction can significantly reduce the electrical resistance of the junction and thereby reduce the amounts of dopants needed. Further-

more, the numbers and shapes of the quantum wells constitute additional degrees of freedom in design that can be used to tailor carrier-transport and potential profiles to optimize laser performance.

Going beyond bipolar cascade lasers, the present innovation could also be

beneficial in some light-emitting diodes and single-stage semiconductor lasers that contain Esaki tunnel junctions. For example, quantum wells could be incorporated into vertical-cavity surface-emitting lasers, wherein Esaki tunnel junctions are used to connect n-doped mirrors to avoid the use of p-doped resistive mirrors.

This work was done by Rui Q. Yang and Yueming Qiu of Caltech for NASA's Jet Propulsion Laboratory. Further information is contained in a TSP (see page 1).

In accordance with Public Law 96-517, the contractor has elected to retain title to this invention. Inquiries concerning rights for its commercial use should be addressed to:

*Innovative Technology Assets Management
JPL*

*Mail Stop 202-233
4800 Oak Grove Drive
Pasadena, CA 91109-8099
(818) 354-2240*

E-mail: iaoffice@jpl.nasa.gov

Refer to NPO-40195, volume and number of this NASA Tech Briefs issue, and the page number.

Phytoplankton-Fluorescence-Lifetime Vertical Profiler

A compact, battery-powered instrument measures marine chlorophyll fluorescence at depths ≤ 300 m.

Stennis Space Center, Mississippi

A battery-operated optoelectronic instrument is designed to be lowered into the ocean to measure the intensity and lifetime of fluorescence of chlorophyll A in marine phytoplankton as a function of depth from 0 to 300 m. Fluorescence lifetimes are especially useful as robust measures of photosynthetic productivity of phytoplankton and of physical and chemical mechanisms that affect photosynthesis. The knowledge of photosynthesis in phytoplankton gained by use of this and related instruments is expected to contribute to understanding of global processes that control the time-varying fluxes of carbon and associated biogenic elements in the ocean.

The concentration of chlorophyll in the ocean presents a major detection challenge because in order to obtain accurate values of photosynthetic parameters, the intensity of light used to excite fluorescence must be kept very low so as not to disturb the photosynthetic system. Several innovations in fluorometric instrumentation were made in order to make it possible to reach the required

low detection limit. These innovations include a highly efficient optical assembly with an integrated flow-through sample interface, and a high-gain, low-noise electronic detection subsystem. The instrument also incorporates means for self-calibration during operation, and electronic hardware and software for control, acquisition and analysis of data, and communications. The electronic circuitry is highly miniaturized and designed to minimize power demand. The instrument is housed in a package that can withstand the water pressure at the maximum depth of 300 m.

A light-emitting diode excites fluorescence in the sample flow cell, which is placed at one focal point of an ellipsoidal reflector. A photomultiplier tube is placed at the other focal point. This optical arrangement enables highly efficient collection of fluorescence emitted over all polar directions. Fluorescence lifetime is measured indirectly, by use of a technique based on the same principle as the one described in "Fluorometer for Analysis of Photosynthesis in Phyto-

plankton" (SSC-00110), *NASA Tech Briefs*, Vol. 24, No. 1 (November 2000), page 79. The excitation is modulated at a frequency of 70 MHz, and the phase shift between the excitation light and the emitted fluorescence is measured by a detection method in which the 70-MHz signal is down-converted to a 400-Hz signal. The fluorescence lifetime can be computed from the known relationship among the fluorescence lifetime, phase shift, and modulation frequency.

In operation, the instrument measures fluorescence intensity and lifetime repeatedly, according to a schedule established during an instrument set-up process, in which the instrument is connected to a host computer. Once programmed, the instrument is disconnected from the computer and remains in a quiescent state as it is placed in the ocean. The measurement process is started by use of a magnetically actuated switch. Measurements taken by the instrument are recorded in a memory module that can hold the data from more than 28,000 measurements. The

set of data from each measurement is time-stamped and includes a pressure/depth datum. Switching the instrument off terminates the series of measurements and prepares the instrument for the next series of measurements. At the end of a series of measurements, the instrument is reconnected to the host computer and the measurement data

are uploaded from the instrument's memory module to the computer.

*This work was done by Salvador M. Fernandez, Ernest F. Guignon, and Ernest St. Louis of Ciencia, Inc., for **Stennis Space Center**.*

In accordance with Public Law 96-517, the contractor has elected to retain title to this invention. Inquiries concerning

rights for its commercial use should be addressed to

Ciencia, Inc.

111 Roberts Street, Suite K

East Hartford, CT 06108

Refer to SSC-00184-1 , volume and number of this NASA Tech Briefs issue, and the page number.

Hexagonal Pixels and Indexing Scheme for Binary Images

For some purposes, this scheme is superior to rectangular pixels.

Lyndon B. Johnson Space Center, Houston, Texas

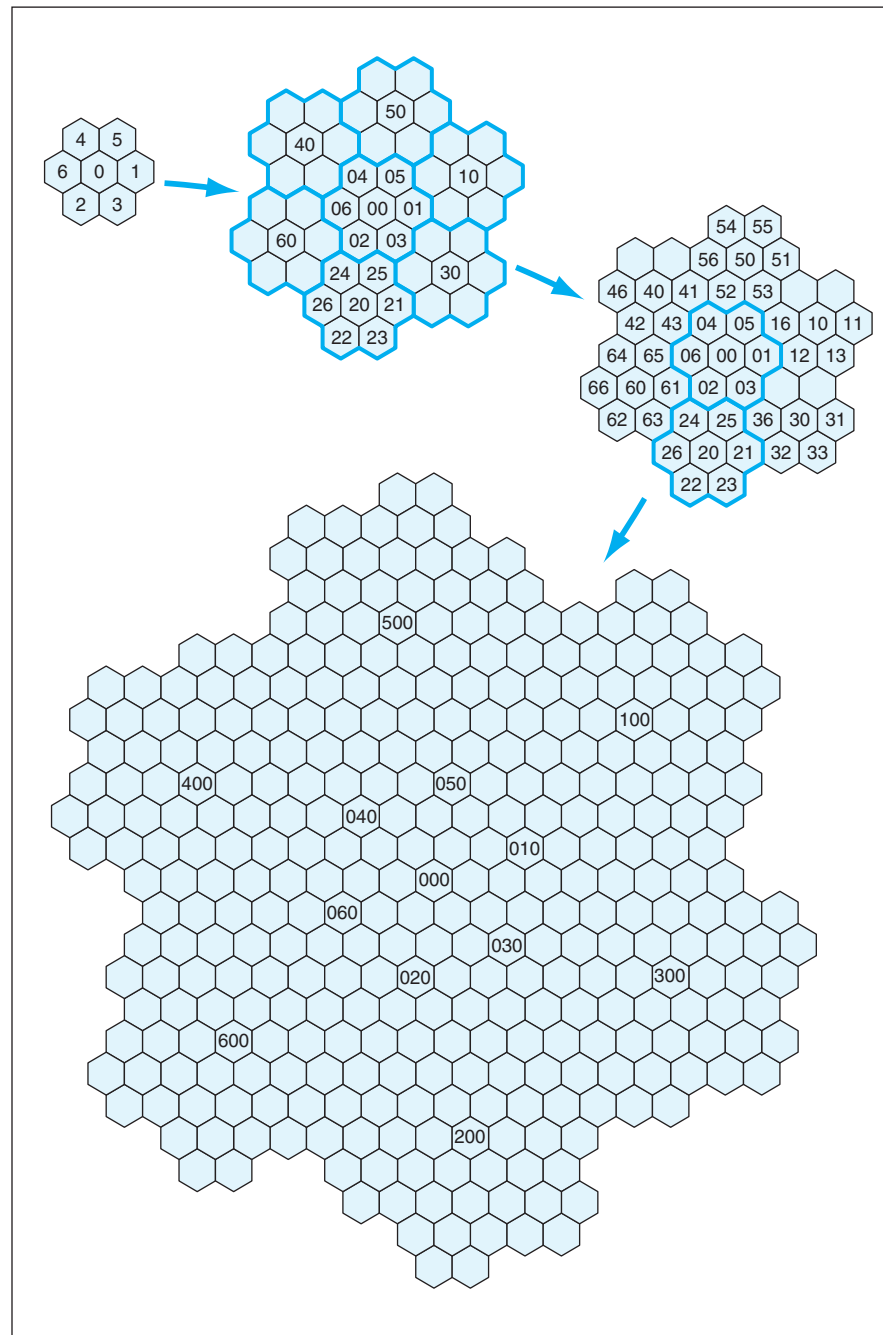
A scheme for resampling binary-image data from a rectangular grid to a regular hexagonal grid and an associated tree-structured pixel-indexing scheme keyed to the level of resolution have been devised. This scheme could be utilized in conjunction with appropriate image-data-processing algorithms to enable automated retrieval and/or recognition of images. For some purposes, this scheme is superior to a prior scheme that relies on rectangular pixels: one example of such a purpose is recognition of fingerprints, which can be approximated more closely by use of line segments along hexagonal axes than by line segments along rectangular axes. This scheme could also be combined with algorithms for query-image-based retrieval of images via the Internet.

A binary image on a rectangular grid is generated by raster scanning or by sampling on a stationary grid of rectangular pixels. In either case, each pixel (each cell in the rectangular grid) is denoted as either bright or dark, depending on whether the light level in the pixel is above or below a prescribed threshold. The binary data on such an image are stored in a matrix form that lends itself readily to searches of line segments aligned with either or both of the perpendicular coordinate axes.

The first step in resampling onto a regular hexagonal grid is to make the resolution of the hexagonal grid fine enough to capture all the binary-image detail from the rectangular grid. In practice, this amounts to choosing a hexagonal-cell width equal to or less than a third of the rectangular-cell width. Once the data have been resampled onto the hexagonal grid, the image can readily be checked for line segments aligned with the hexagonal coordinate axes, which typically lie at angles of 30° , 90° , and 150° with respect to say, the horizontal rectangular coordinate axis. Optionally, one can then rotate the rectangular image by 90° , then again sample onto the hexagonal grid and check for line

segments at angles of 0° , 60° , and 120° to the original horizontal coordinate axis. The net result is that one has checked for line segments at angular

intervals of 30° . For even finer angular resolution, one could, for example, then rotate the rectangular-grid image $\pm 45^\circ$ before sampling to perform



The **Tree-Structured Indexing Scheme** provides information on both locations and levels of resolution. In each group of seven pixels that constitute one pixel at the next coarser level of resolution, the zeroth pixel is the central one.

checking for line segments at angular intervals of 15° .

In the tree-structured pixel-indexing scheme, the smallest hexagonal pixels in nearest-neighbor groups of seven constitute larger pixels, which, in turn, are grouped into still larger pixels (see figure), and so forth, proceeding from the finest resolution to the coarsest. Each pixel is identified by a sequence of integers in order of increasing resolution. In other words, the first integer in an address denotes the coarsest pixel

that contains the location in question, the second integer denotes whichever one of the seven subpixels of the coarsest pixel contains the location of interest, and so forth down to the last integer, which denotes the smallest hexagonal cell that contains the location of interest.

For some purposes — especially performing quick searches for images that match query images, it is useful to resample a binary image data from finer hexagonal grids onto coarser hexagonal

grids. In such a case, each pixel at the next coarser level of resolution is made exactly hexagonal and considered dark if more than three of its seven component pixels are dark.

This work was done by Gordon G. Johnson of the University of Houston for Johnson Space Center. For further information, contact the Johnson Commercial Technology Office at (281) 483-3809. MSC-22901

Σ Finding Minimum-Power Broadcast Trees for Wireless Networks Algorithms for identifying viable trees have been derived.

NASA's Jet Propulsion Laboratory, Pasadena, California

Some algorithms have been devised for use in a method of constructing tree graphs that represent connections among the nodes of a wireless communication network. These algorithms provide for determining the viability of any given candidate connection tree and for generating an initial set of viable trees that can be used in any of a variety of search algorithms (e.g., a genetic algorithm) to find a tree that enables the network to broadcast from a source node to all other nodes while consuming the minimum amount of total power. The method yields solutions better than those of a prior algorithm known as the broadcast incremental power algorithm, albeit at a slightly greater computational cost.

It is not possible to give more than a highly abbreviated and oversimplified summary of the method within the space available for this article. However, to give meaning to even this brief summary, it is necessary to present some details of the underlying rules, simplifying assumptions, and mathematical constructs in the following two paragraphs.

Each node is equipped with an omnidirectional antenna. The minimum transmitter power that enables the j th node to send information to the i th node is proportional to r_{ij}^α where r_{ij} is the distance from node j to node i and α is a channel-loss exponent that usually lies between 2 and 4, the exact value depending on the nature of the signal-propagation medium. Any node in a network can be used to relay a signal to any other node. For the purposes of this method, only the transmitter power levels are calculated: the

receivers are assumed to draw negligible power.

For a network of N nodes, one constructs a power or cost matrix, which is an N -by- N matrix \mathbf{P} , of which each element P_{ij} is proportional to the minimum power needed for communication between nodes i and j as described above. To represent connections between nodes of the network, one uses an N -element vector, denoted a cut vector, each element of which represents the location of an element in a row of the power matrix. Associated with each cut vector is a threshold vector, the elements of which are the power-matrix elements picked out by the cut vector. The cost of a cut is defined as the sum of the elements of the threshold vector. A cut is regarded as viable if it enables a broadcast to reach all nodes; otherwise, it is regarded as not viable. Another means of characterizing the network is the transfer matrix, which is an N -by- N matrix that is a function of the threshold vector.

One element of the present method is a construct denoted the viability lemma, which provides a necessary and sufficient condition for a cut to be viable. The viability lemma is implemented by equations that require power operations on the transfer matrix. In the case of a large network, power operations on a matrix can be computationally expensive. An alternative algorithm for determining viability does not require matrix power operations; instead, it requires an iterative procedure that involves examination of the rows of the transfer matrix and that is guaranteed to reach an indication of

either viability or non-viability in $N - 1$ or fewer iterations.

Another element of the present method is the connection matrix, which is a binary N -by- N matrix representation of a tree. The connection matrix is built iteratively from a cut that has been found to be viable by one of the means described above.

Yet another element of the present method is a stochastic tree-generation algorithm that can be used to generate a viable cut vector. This is an iterative algorithm that starts with a transmission from the source node to a randomly chosen destination node, followed by heuristic selection of the next destination node at each subsequent iteration, until all intended destination nodes are reached. This algorithm converges in $N - 1$ or fewer iterations.

This work was done by Payman Arabshahi, Andrew Gray, Arindam Das, Mohammed El-Sharkawi, and Robert Marks II of Caltech for NASA's Jet Propulsion Laboratory. Further information is contained in a TSP (see page 1).

In accordance with Public Law 96-517, the contractor has elected to retain title to this invention. Inquiries concerning rights for its commercial use should be addressed to

Intellectual Assets Office

JPL

Mail Stop 202-233

4800 Oak Grove Drive

Pasadena, CA 91109

(818) 354-2240

E-mail: ipgroup@jpl.nasa.gov

Refer to NPO-30455, volume and number of this NASA Tech Briefs issue, and the page number.

Automation of Design Engineering Processes

A method facilitates ISO 9001 compliance and eliminates voluminous, difficult-to-manage paper files.

John F. Kennedy Space Center, Florida

A method, and a computer program that helps to implement the method, have been developed to automate and systematize the retention and retrieval of all the written records generated during the process of designing a complex engineering system. It cannot be emphasized strongly enough that “all the written records” as used here is meant to be taken literally: it signifies not only final drawings and final engineering calculations but also such ancillary documents as minutes of meetings, memoranda, requests for design changes, approval and review documents, and reports of tests.

One important purpose served by the method is to make the records readily available to all involved users via their computer workstations from one computer archive while eliminating the need for voluminous paper files stored in different places. Another important purpose served by the method is to facilitate the work of engineers who are charged with sustaining the system and were not involved in the original design decisions. The method helps the sustaining engineers to retrieve information that enables them to retrace the reasoning that led to the original design decisions, thereby helping them to understand the system better and to make informed engineering choices pertaining to maintenance and/or modifications of the system.

The software used to implement the method is written in Microsoft Access. All of the documents pertaining to the design of a given system are stored in one relational database in such a manner that they can be related to each other via a single tracking number. In addition to improving the management of records of the design process, the method can be utilized to improve the design process itself in a number of ways that include the following:

- Any component of the total collection of design data can be retrieved immediately.
- Through careful construction of the portion of the software that governs the inputs to the database, one can tailor the design process so that the software prompts for all required inputs, thereby ensuring that required components of the system are not overlooked.
- The software provides that a given data element can be entered once and is then automatically reused as needed, eliminating the need for repetitive typing and eliminating the confusion caused by differences among different textual entries of essentially the same information.
- Inputs can be constructed easily. For system designs requiring similar inputs, relatively simple cut-and-paste operations can be performed.
- Fewer than the customary administra-

tive procedures are needed. Most of the instructions on how to supply the requested information can be provided by the software in the form of help screens.

- The design process can be quickly and efficiently integrated in the sense that different engineering and administrative disciplines and design subprocesses can be tied together and the relevant information made available to all persons monitoring the database.
- The aforementioned integration is enforced by requiring feedback from design subprocesses in different disciplines.
- It facilitates ISO 9001 compliance through a structured design process, which includes objective evidence of meeting requirements.
- Metrics for the entire design process can be built into each process step and displayed.
- The quality of the final product is improved through reduction of the probability of missing design-process steps.
- Scheduling is included in the integration and is thereby enhanced.

*This work was done by Glenn Torrey, Gerald Sawasky, and Karim Courey of United Space Alliance for Kennedy Space Center. Further information is contained in a TSP (see page 1).
KSC-12294*



National Aeronautics and
Space Administration